Research paper

A comprehensive review on scour and scour protections for complex bottom-fixed offshore and marine renewable energy foundations

J. Chambel [a,b,*], T. Fazeres-Ferradosa [a,b], F. Miranda [a,b], A.M. Bento [a,b], F. Taveira-Pinto [a,b], P. Lomonaco [c]

[a] Hydraulics, Water Resources, And Environmental Division, Department of Civil Engineering, Faculty of Engineering of the University of Porto, 4200-465 Porto, Portugal
[b] Interdisciplinary Centre of Marine and Environmental Research of the University of Porto (CIIMAR), 4450-208 Matosinhos, Portugal
[c] O.H Hinsdale Wave Research Laboratory, College of Engineering, Oregon State University, Corvallis, OR, United States

ARTICLE INFO

ABSTRACT

Due to the marine environment's complexity, optimising offshore foundations' design is still a major focus of the scientific and industrial community, since foundations represent a large portion of the total investment. Scour is one of the main causes that lead to ultimate, and service limit states, impacting design optimization and costs. Scour at monopile foundations has been extensively studied. However, advances in scour protections for hybrid structures, and other bottom-fixed foundations for offshore renewable energy harvesting technologies are often kept confidential by stakeholders, and knowledge gaps must be covered. Thus, the present paper provides a summary of the most recent physical and numerical studies related to scour and riprap scour protections for complex bottom-fixed foundations, such as jackets, tripods, gravity-based foundations (GBF), high-rise structure foundations (HRSF), and suction buckets, while covering other marine energy harvesting technologies as well, including wave energy converters (WEC) and tidal energy converters (TEC). This manuscript presents knowledge gaps, recent improvements, and potential studies on hybrid foundations – offshore wind turbine foundations combined with WECs or TECs. It is shown that offshore scour protection is a study field with a wide margin of development, but crucial for the future of the offshore renewable energy sector, thus pointing out key challenges and major opportunities for future research.

1. Introduction

As one of the most attractive forms of clean energy, the offshore wind energy sector (OWS) has been seen as an important part of the future of renewables and energy transition, particularly given the European efforts and policies towards net-zero carbon emissions, to be achieved by 2050 (WindEurope, 2021a). OWS has experienced an increase in demand due to the expansion and competitiveness of the sector, with more efficient and mature technology, and a continuous reduction of the Levelized Cost of Energy (LCoE).

In bottom-fixed Offshore Wind (OW), the foundation is typically responsible for around 30% of the overall investment (Matutano et al., 2013; Bhattacharya, 2014), and an essential part of that investment is allocated to scour protection (Fazeres-Ferradosa et al., 2019a). Due to the complexity of the offshore environment, understanding the impact that entails the foundation and protection design is vital for design optimization purposes of those two structural components, causing a

positive impact on the decrease of global investment and the LCoE. Scour protections are one of the preferential contributors to achieving a cost reduction given the empirical nature of its design. Over the past decade, scour protection solutions have registered major advances, and could potentially be applied to complex foundations, wave/tidal energy converters, and eventually offshore hybrid foundations as well (Fazeres-Ferradosa et al., 2021).

It is expected that by 2030, bottom-fixed and floating offshore wind turbines will experience an LCoE reduction of 44%–48 €/MWh and 65% to 69 €/MWh, respectively, when compared to 2020, far less from the 150 €/MWh value of the 2010s (WindEurope, 2021a, 2022a). To reach climate neutrality, wind energy needs to cover 25% of European Union (EU) demands by 2030 and 50% by 2050 (17% of them being OWS) with 81% renewables (WindEurope, 2021a). In the short period, it will be necessary for a total wind energy capacity of 453 GW–79 GW of OWS (WindEurope, 2022b). To attain that mark is imperative to install, between 2022 and 2026, at least 27.9 GW of offshore wind, nearly 8.5

GW/year – significantly different from the 3.4 GW installed in 2021 (WindEurope, 2022b).

The implementation of some of the developments and novel design methods for scour protections is kept private by most of the industrial stakeholders. However, some topics need to be addressed, that can have a major influence on optimized designs, such as the scour patterns and scour protections for complex foundations and new geometries; the impact that WECs or TECs produce on the flow field, seabed, and protections; effects that offshore wind turbine lifetime cycle extension can cause on existing foundations; or effects that repowering or more powerful turbines can or should have on the dimensions of the foundations and consequently in the design of the scour protections (Fazeres-Ferradosa et al., 2021).

The challenges, trends, and knowledge gaps regarding offshore scour protections and foundations ask for an uninterrupted research effort by the scientific community. Therefore, this article presents a review of the latest outcomes of scour protections applied in complex bottom-fixed structures for offshore wind and marine energy harvesting technologies. It aims to encapsulate the existing knowledge and most recent research performed on offshore foundations' scour protection, from monopiles to more complex and hybrid foundations, and point out potential research fields and synergies.

The paper is organized as follows: Section 2 briefly references the most recent design methodologies and optimizations of scour protections. Section 3 provides a broad review of the latest findings in scour and scour protections for complex structures (jackets, tripods, and GBFs), referencing different physical and numerical model studies. Section 4 gives a general insight into marine energy harvesting technologies such as wave energy converters, tidal energy converters, and hybrid foundations. Finally, in Section 5, some conclusions, knowledge gaps, and future research lines are highlighted.

2. Offshore scour protection design methodologies

Offshore structures are used for multiple purposes. Some of them are implemented in fixed platforms, others in floating platforms, such as production, storage, offloading platforms, oil/gas rigs, offshore high voltage stations (OHVS), and offshore wind turbines (OWT) – Amaechi et al. (2022) and Haritos (2007).

Regarding OWTs, their foundations can have different configurations and can be placed in a wide range of water depths, thus being divided into two major groups.

- **Bottom-fixed foundations:** foundations fixed on the seabed. Monopiles are the most used, placed mainly in shallow waters (until 30 m deep). Other, and more complex foundations, such as jackets, tripods, GBFs, and Suction Buckets are better suited for transitional waters (until 50–60 m deep) – Fig. 1. Recently, a new type of complex foundation, the High-Rise Structure Foundation (HRSF), has been

gaining some momentum and has been often used in Asian offshore wind farms - Fig. 2;

- **Floating offshore wind turbines (FOWT):** OWT with floating platforms attached to the seabed by mooring lines and anchors, including barge, semi-submersibles, Spar buoys, and tension leg platforms (TLPs).

Only 18.5% of the OWT foundations in Europe are complex bottom-fixed foundations (Fig. 3) – jackets (9.9%), GBFs (5%), tripods (2.2%), and tripile (1.4%), WindEurope (2021b).

OWT might be placed in movable seabeds with either cohesive or non-cohesive properties. The offshore conditions can vary significantly, so the structure foundations' presence induces considerable flow changes. The interactions between the flow and the structure, increase the bed shear stress, since local velocities increase, as well as flow-induced turbulence, thus initiating sediment transport. When the critical bed shear stress is exceeded, the scouring process begins (Sumer et al., 2001; De Vos et al., 2011; Whitehouse et al., 2011a; Sørensen and Ibsen, 2013). So, scour can be defined as the generalized erosion of the seabed in the structure surrounding area, as a result of the interaction between the soil, flow, and structure. It is the leading cause of structural failure by ultimate or service-limit states. Hence, scour protections play a critical role in the OWT design and overall costs. For bottom-fixed foundations, scour protections are placed around the foundation. Conversely, at FOWT scour protections should be established around elements that are more exposed to scour such as drag-embedment anchors (DEA) and their associated subsea structures such as tensioners, clump weights, and chains (Sumer and Kirca, 2022).

Fig. 2. High-Rise Structure Foundation (HRSF), Reprinted with permission from Xiao et al. (2020), Copyright 2020, Elsevier.
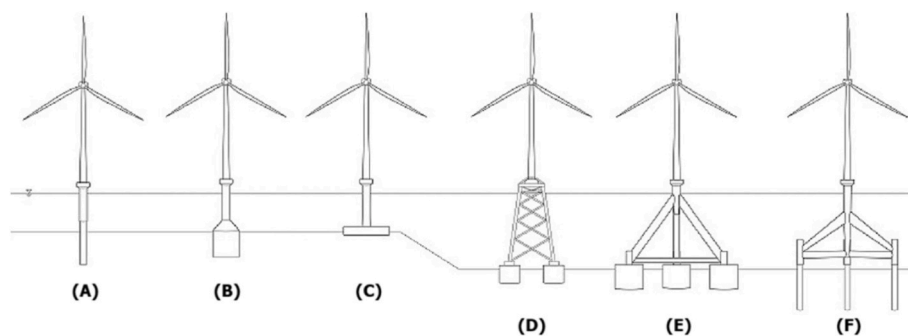

Fig. 1. Bottom-Fixed Foundations: (A) Monopile, (B) Monopile with Suction Bucket, (C) Gravity-Based Foundation, (D) Jacket with Suction Bucket, (E) Tripod with Suction Bucket, (F) Tripod – adapted from Bhattacharya (2014).
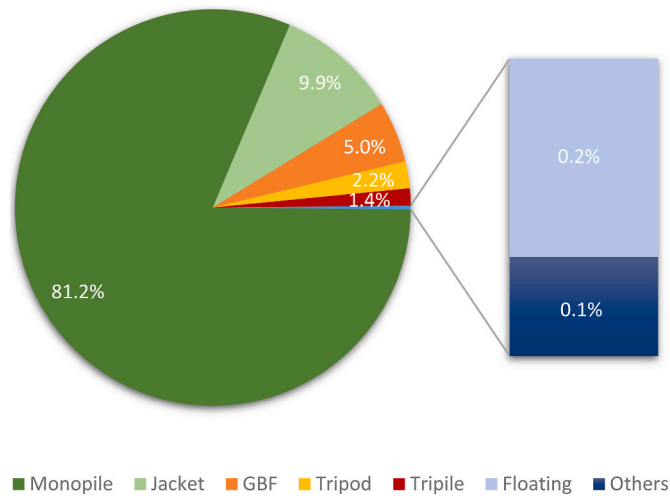
Fig. 3. – Offshore wind foundations installed in Europe by type (WindEurope, 2021b).

2.1. Scour countermeasure classification

As scour develops around the foundation, the overall structural response changes regarding the serviceability, eigenfrequency, and fatigue limit state. Scour protections must be designed to prevent erosion of the seabed sediments while preserving permeability to prevent larger pore pressure increments, allowing seepage water drainage (Saathoff et al., 2024). Moreover, scour protections can have a positive impact on the foundation's stiffness (up to a 50% increase), Saathoff et al. (2024). However, different protective measures have different costs and they are highly susceptible to location, material size, availability, transport, and installation, as well as to marine environmental conditions, including water depth, wave characteristics, current velocity and direction, wave-current interaction, tides, storm surges, and storm durations, among others (Fazeres-Ferradosa et al., 2021; Chambel, 2019). Different studies have been performed for distinct scour countermeasures (Fazeres-Ferradosa et al., 2019b; Vahdati et al., 2020; Corvaro et al., 2018). According to Li et al. (2023), Zhang et al. (2023), and Tang et al. (2022), there are two major groups of scour countermeasures.

- **Passive protections:** the most common countermeasure. Used to control or reduce scour by strengthening the seabed sediment particles or by using armouring structures around the foundation. They are known for their cost-effectiveness and ease of application. Riprap

protection and rockbags are probably the two most used solutions in offshore wind farms;

- **Active protections:** passive countermeasures require maintenance and could have a certain life span due to aggressive offshore conditions, leading to structural failure in some cases. Therefore, active countermeasures became in demand, as they intend to reduce scour by altering the flow patterns around the foundation and/or by reducing the flow intensity. Within the most known it can be highlighted systems like collars, vanes, and sacrificial piles.

Furthermore, a third classification (comprehensive protection) was introduced by Zhang et al. (2023), to categorize countermeasures that incorporate both active and passive protections or scour protections that combine or use additional biological or eco-friendly components. Fig. 4 encapsulates the overall range of possible scour mitigation measures that can be applied in the offshore, marine, and fluvial environments.

2.2. RipRap scour protections

Riprap protections, inspired by rubble-mound breakwaters, placed around the foundation (Fig. 5), are the most common solution due to their high availability and low cost (Fazeres-Ferradosa et al., 2019a; De Vos, 2008). It was demonstrated by Ma and Chen (2021) and Yin et al.
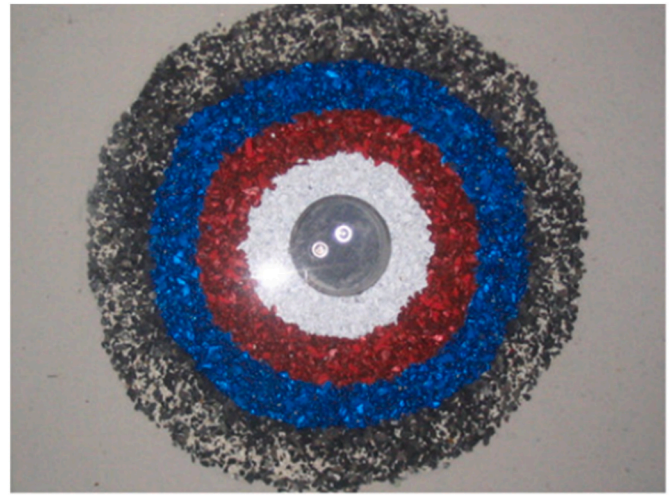

Fig. 5. Riprap scour protection model for a monopile – Adapted and Reprinted with permission from De Vos et al. (2011). Copyright 2011, Elsevier.
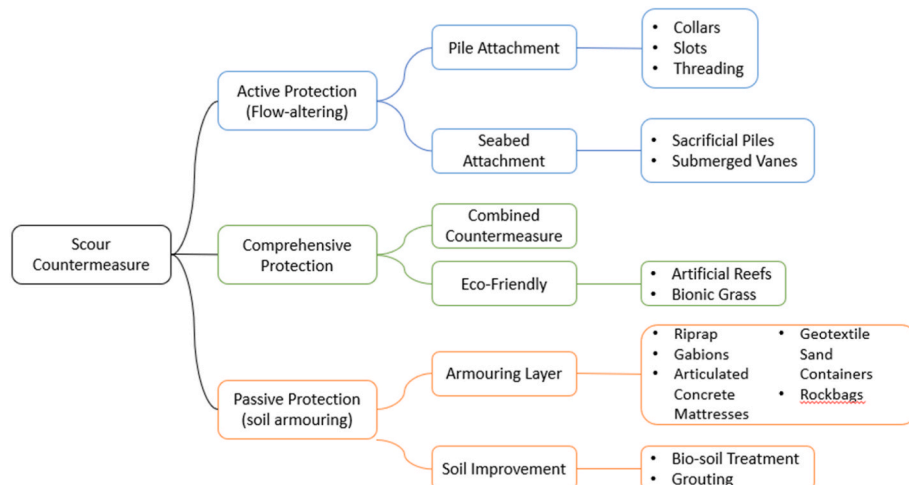

Fig. 4. Scour countermeasures classification according to Li et al. (2023), Zhang et al. (2023), and Tang et al. (2022).

(2023) that they enhance the structural behaviour of the foundation as they could decrease the cross-sectional rotation up to 18% in a service-limit state, but also improve the foundation's reliability index, thus having a positive effect on the ultimate limit state.

According to De Vos et al. (2011, 2012) and Schendel (2018), they are usually classified as follows.

- **Static protections:** the movement of the elements of the armour layer is not allowed. This is the most common type of protection used in commercial offshore wind projects (Fazeres-Ferradosa et al., 2021). The static design is based on the threshold of motion concept, which states that the critical stone size (D_{cr}) should be determined so that the shear stress induced by environmental conditions is smaller than the critical shear stress of the material (Soulsby, 1997). The most common design formula (Equation (1)) was presented in Soulsby (1997), where the mass density of the material (ρ_s) directly impacts the median stone size ($D_{50}=D_{cr}$) used – where τ_{cr} (N/m^2) is the critical bed shear stress, ρ_w (kg/m^3) is the water mass density, and θ_{cr} is the critical Shields parameter, which for non-cohesive soils a dimensionless grain size (D^*) larger than 100 has an asymptotic value of 0.056, Soulsby (1997).

$$\tau_{cr} = \theta_{cr}g(\rho_s - \rho_w)D_{50} \tag{1}$$

$$D^* = \left(\frac{g(s-1)}{v^2}\right)^{1/3}d_s \tag{2}$$

When applied to monopiles or other complex foundations, an amplification factor, the ratio of disturbed over undisturbed bed shear stress, is included to consider the effect that the bottom-fixed foundations produce on the increase of wave-current shear stress. For monopiles, amplification factors were studied by Whitehouse (1998) and Sumer and Fredsøe (1997). However, those amplification factor values cannot be extrapolated for complex structures. Therefore, the static design of scour protections and the adequate values of the amplification factor for complex foundations represent a considerable knowledge gap.

- **Dynamic protections:** a controlled movement of the elements of the armour layer is allowed. Although not extensively used in commercial offshore projects, or at least not publicly disclosed, they have been the scientific community's focus for the last 18 years, and represent an upgrade to static protections, in the sense that allows for a reduction of the median stone size of the armour. Design formulas have been studied and proposed by De Vos (2008) and De Vos et al. (2012). Still, the first studies mentioning dynamic protections were conceived in the OPTI-PILE project by den Boon et al. (2004), where the threshold of motion ceased to be the criteria for the design. Instead, De Vos (2008) and De Vos et al. (2012) developed a new design approach that defined failure when the filter layer is exposed in an area equivalent to $4.5D_{n50}^2$ – comparable to a square of two-by-two D_{n50} stones. A damage number (S_{3D}) equation was proposed De Vos (2008) and De Vos et al. (2012), based on the breakwaters formula of Van Der Meer (1990), Equation (3), allowing the protections' classification into three different levels of damage: static ($S_{3D} < 0.25$), dynamic ($0.25 < S_{3D} < 1.00$), and failure ($S_{3D} \geq 1.00$).

$$\frac{S_{3D}}{N^{b0}} = a_0 \frac{U_m^3 T_{m-1.0}^2}{\sqrt{gd}(s-1)^{3/2}D_{n50}^2} + a_1\left(a_2 + a_3\frac{(U_c/w_s)^2(U_c + a_4U_m)^2\sqrt{d}}{gD_{n50}^{3/2}}\right) \tag{3}$$

where N is the number of waves, g (m/s^2) is the gravitational acceleration, d (m) is the water depth, U_m (m/s) is the orbital velocity, $T_{m-1,0}$ (s) is the energy wave period, s is the ratio between ρ_s and ρ_w, U_c (m/s) is the depth-average velocity, w_s (m/s) is the settling velocity, a_0, a_2, a_3 and b_0 are regression coefficients equal to 0.00076, −0.022, 0.0079 and 0.243, respectively, and a_1 and a_4 are coefficients for hydrodynamic conditions defined in De Vos (2008) and De Vos et al. (2012).

Opposite to the static design method, the dynamic design equation does not rely on the amplification factor. When compared to static protections, dynamic ones typically have a decreased stone size (D_{n50}) and thickness (Table 1), which is expected to lead to smaller material, transportation, and installation costs (Matutano et al., 2013). However, an excessive reduction of D_{n50}. Can still lead to thicker armour layers to sustain damage without failure, eventually increasing costs (Fazeres-Ferradosa et al., 2021). Therefore, a balanced solution is required for practical optimization. Furthermore, like static protections, most studies only considered monopile foundations and a short variety of water depths and layer thicknesses. Therefore, in the application of dynamic scour protections to complex foundations, there is a large knowledge gap yet to be fully covered.

- **Wide-graded protections:** single-layer protections formed by wide-graded material that simultaneously plays the role of armour and filter, and that can have a static or dynamic behaviour. Several researchers (Schendel, 2018; Schendel et al., 2014, 2016, 2018) performed studies and optimized this type of protection. They consensually registered an overall stability increase, when compared to narrow-graded protections. Such stability is pointed out as a result of the sheltering of smaller stones between the voids of larger ones. Wide-graded protections are almost static under currents, rather than under waves in which they tend to be dynamically stable when compared to other protections with the same D_{50}, Schendel et al. (2014). For static wide-graded protections, the design formula (Equation (4)) was presented by De Vos et al. (2011):

$$\tau_{cr} = \theta_{cr}g(\rho_s - \rho_w)D_{67.5} \tag{4}$$

where $D_{67.5}$ and $\theta_{cr} = 0.035$ are used instead of D_{50} and $\theta_{cr} = 0.056$, so the τ_{cr} for wide-graded protections will be larger than for narrow-graded protections, for the same D_{50} value (De Vos et al., 2011).

For dynamic wide-graded protections, the dynamic design formulas do not apply since they are based on a filter exposure that does not exist in wide-graded protections. They can be an appealing type of protection, from the stability, material availability, installation, and cost point of view in some cases. The literature reveals, however, a lack of dynamic design formulas specifically developed for wide-graded single-layer scour protections, both for monopiles and for complex foundations. Also, there is a lack of reported experimental data, tests, and results, as well as field applications. Thus, wide-graded protections still represent a concept whose efficiency is yet to be fully understood.

In terms of efficiency, Wang et al. (2023a) compared the scour depth obtained from an unprotected monopile to a monopile protected with riprap static and dynamic protections. The results showed a maximum scour depth reduction of 26.1% (static), 73.8% (dynamic single-layered), and 86.9% (2-layered dynamic protection), respectively. However, for clarity, the tests were performed using only steady currents. Nonetheless, the results are a good indication that not only dynamic protections can be cheaper, but they can also have higher performance on counteracting scour.

2.3. Alternative passive scour protections

Regarding other scour countermeasures, this review focuses primarily on riprap scour protections. However, a brief mention will be made of solutions with an armouring effect around the foundation. A more extensive review of other alternative protective systems can be found in Li et al. (2023), Zhang et al. (2023) and Tang et al. (2022), as they are not the focus of this review. The studies found in the literature, regarding armouring and strengthening scour mitigation systems, mention mainly partial grouting, gabions, articulated concrete mattresses (ACM), and geotextile sand containers (GSC). They are usually implemented to counter scour in bridges, river slopes, and nowadays in offshore wind farms (Li et al., 2023; Zhang et al., 2023; Tang et al.,

Table 1

- D_{50} (m) comparison of different design approaches for the same tested conditions: $d = 20$ m; $H_{m0} = 6.5$ m; $T_p = 11.2$ s; $U_c = 1.5$ m/s; $D_{85/15} = 2.5$ (prototype values) – adapted from De Vos et al. (2011), De Vos (2008), and De Vos et al. (2012).

Static Approach				Dynamic Approach		
Amplification Factor (α_f)	Fredsoe and Deigaard (1992) (use of τ_m)	Soulsby (1997) (use of τ_{max})	De Vos et al. (2011) (Equation (1))	S_{3D} (Equation (3))	De Vos (2008), De Vos et al. (2012) (Waves following Currents)	De Vos (2008), De Vos et al. (2012) (Waves opposing Currents)
2	0.68	0.66	0.496	**0.2**	0.44	0.46
3	1.30	1.51		**0.5**	0.32	0.36
4	1.97	2.75		**1**	0.27	0.28

2022). Recently, new eco-friendly scour protections, such as microbially induced calcium-carbonate precipitation (MICP), Li et al. (2022a, 2022b), ionic soil stabilizers (ISS), Hu et al. (2022a, b), artificial reefs (AR), and bionic grass have been receiving increased interest and relevancy by the scientific community.

- **Partial Grouting:** a method in which the armour layer units are bonded together by special mortar, filling about 50% of the voids, to produce a high-stability layer that lasts longer against scour and has sufficient permeability to avoid excess water pressure below the protection's armour (Li et al., 2023; Zhang et al., 2023; Heibaum et al., 2010). Combines a high resistance against currents and waves with the flexibility to adapt to seabed deformations. According to Heibaum et al. (2010), partial grouting protections proved stability up to flow velocities of 8 m/s in laboratory tests. Zhang et al. (2022) carried out a series of physical model tests using currents, waves, and combined waves and currents to compare an unprotected to a partial grouting monopile foundation. When comparing the grouted to the "ungrouted" model, it was concluded that the critical shear stress needed to initiate scour from the incipient motion of particles in the grouted monopile was 10 times higher when compared to the "ungrouted" monopile. Therefore, for weak hydraulic actions only the unprotected monopile had suffered from scour. However, when strong hydraulic conditions were applied, some cracks and scour holes occurred around the foundation for the grouted protection. Nonetheless, Zhang et al. (2022) concluded that grouting protections could be more efficient under extreme hydrodynamic conditions when compared to riprap protections. To study this possible enhancement, Wang et al. (2023b) performed a series of physical large-scale model tests on grouted riprap protection (Fig. 6a), where the armour layer units were cemented. By applying two extreme

wave-current conditions with return periods of 50 and 100 years, it concluded that the maximum scour depth could be reduced up to 80% when compared to an unprotected monopile;

- **Gabions:** wire sacks, boxes, baskets or mattresses filled with riprap material that are used to improve stability and reduce scour (Li et al., 2023). The gabions are predominantly used on bridges or for the stabilization of river margins as described in Pagliara et al. (2011), Singh et al. (2022), and Agrawal et al. (2007). However, no studies or *in-situ* applications regarding the use of gabions as a scour protection for OWT foundations were found in the literature;

- **Articulated Concrete Mattresses (ACM):** a matrix of concrete connected through wires to form a single protective unit, has the advantage of being manufactured before the OWT installation with rigours and higher control quality (Li et al., 2023). Although not applied directly to an OWT foundation, Coghlan et al. (2023) tested these mats under wave-induced loading for a small-scale model of the monolithic maritime structure of the Port of Hay Point (Australia) – Fig. 6b. The original mats provided seabed scour protection successfully for almost 50 years. However, the results showed that the original degraded mats had insufficient stability under extreme wave conditions, mainly at the caisson corners. Therefore, newly upgraded mats were implemented and successfully tested as new countermeasures. Liang et al. (2022) performed a three-dimensional (3D) numerical model to study the seabed instability around an offshore pipeline under multiple wave-current hydrodynamic loads, when protected by ACMs. The goal was to assess the results while varying the spacing between two consecutive protections and the interaction angle ($\alpha_{wc\text{-}mp}$) – ranging between $0°$ (pipeline perpendicular wave-current load) and $90°$ (pipeline colinear to wave-current load). The results allowed to extract several conclusions: the presence of the protection led to a clear reduction in
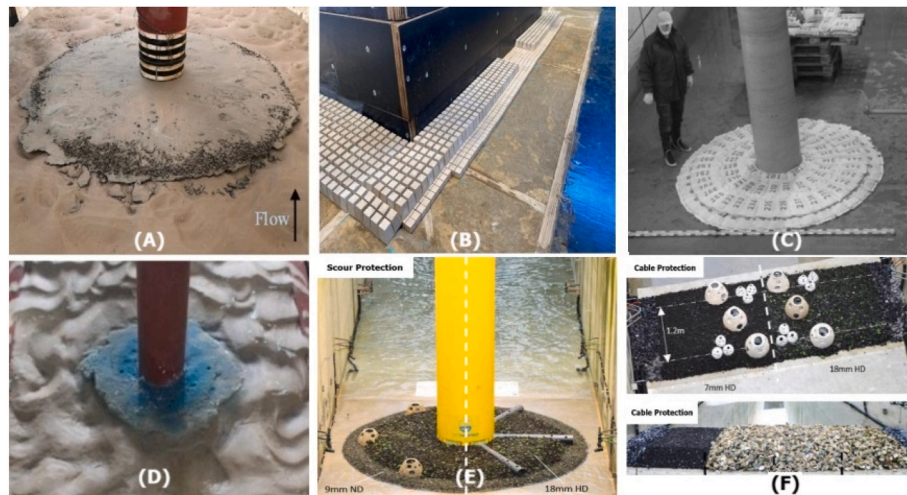
Fig. 6. Alternative scour protection systems: (A) Partial grouted riprap – Reprinted with permission from Wang et al. (2023b), Copyright 2023, Elsevier; (B) Articulated Concrete Mattress (ACM) – adapted from Coghlan et al. (2023); (C) Geotextile Sand Containers (GSC) – adapted from Grüne et al. (2006c); (D) Microbially Induced Calcium-Carbonate Precipitation (MICP) – Reprinted with permission from Li et al. (2022b), Copyright 2022, Elsevier; (E) and (F) Artificial Reefs with oysters/shells – adapted from Aleksandrova et al. (2023).

seabed sediment loss, even along the unprotected sections (around 20%); the drop of the seabed increases from the centre of the ACM protection towards its edge, where instability occurs first; the seabed loss tends to become more severe with the increase of the current velocity; when the mattress spacing exceeds 18 times the pipeline diameter, the loss of sediments in the unprotected area achieves the same range of a pipeline without any protected conditions; wave height and soil permeability were regarded as dominant factors, on behalf of the wave period and seabed saturation, in the stability design of the ACMs-pipeline system on sandy seabed's. However, Liang et al. (2022) suggests that the α_{wc-mp} between the ACMs-pipeline system and the hydrodynamic conditions should be the first factor considered, as the spatial distribution of the seabed sediment loss is considerable when $\alpha_{wc-mp} < 45°$;

- **Geotextile Sand Containers (GSC):** GSCs or geotextiles have been massively used in geotechnical engineering and for coastal protection. Nowadays, some offshore wind farms like the OWP Amrumbank West (Germany) opt for this type of solution as a scour protection (Hoyme et al., 2018). Grüne et al. (2006a, b) proposed GSCs as scour protections for monopiles, to minimize the risk of damage to the offshore foundation and the cables during the construction period. The physical model program started to investigate the GSCs' stability to inline and transverse wave-induced currents, by testing 4 GSC sizes for 3 percentages of filling, resulting in 12 different container weights. The results showed that the stability of the containers is not just a function of the total weight, but also the wave directions and percentage of filling. The experimental data have shown that increasing the percentage of filling resulted in increasing stability, *i.e.*, GSCs with lower weight and higher percentage of filling are more stable than GSCs with higher weight and low percentages of filling. The decrease in stability was attributed to the increasing acting forces from the hydrodynamic loads because of the successive changes in the shape of the container due to the interior movement of the sand particles. As a follow-up, Grüne et al. (2006c) performed a large-scale model of complete scour protections around a monopile (Fig. 6c), by comparing two GSCs' placement configurations (regular and irregular). After different test series of 2000–3000 waves, in which the wave height and peak period were increased stepwise, displacements above 5% were registered for the maximum significant wave height (1.0 m). The main results indicate that no significant differences were found in terms of stability, considering both configurations of the scour protection. For irregularly placed GSCs, at the beginning, a self-adjustment process of the protection occurs. However, when the displacement of the containers starts, the process continues to occur much faster for "regular" scour protection compared to "irregular" scour protection. Corvaro et al. (2018) carried out experimental tests with regular and irregular waves to assess the performance of scour protections made of 80%-filled GSCs around a monopile. Several configurations (circular, two configurations with different orientations of the containers, and random) were tested and compared to an unprotected monopile. Corvaro et al. (2018) mentions that GSC scour protections have two major failure modes, sliding and overturning, being the second mode the main mechanism. The results showed that, generally, damage for regular waves achieved an equilibrium stage for 500 waves, while for irregular waves that condition was obtained for 1500 waves. Moreover, the squared configuration presented the best (long edge following the wave direction) and worst result (long edge transversal to wave direction) in terms of efficiency, thus showing that the wave direction has a strong influence on the protection's performance. Additionally, for the random configuration significant displacements were observed at the beginning due to the initial random arrangement to a more stable position. Hence, Corvaro et al. (2018) concluded that GSC scour protections reduce massively scour depths, as no failure, scour, or significative sinking/overturning was observed even for waves with large heights and peak periods, and

that the circular configuration represents the best overall solution. As a novel contribution, it developed and presented a new dynamic design formula, Equation (5a), for the determination of the container's weight based on an adaptation of the stability number (N_s) of Hudson (1959):

$$N_s^* = N_s \bullet k_1 \bullet \frac{H}{d} = \frac{H^2}{\Delta \bullet l} \bullet k_1 \tag{5a}$$

$$l = \left(\frac{W}{k_w \gamma}\right)^{1/3} \tag{5b}$$

being $N_s \times$ the modified stability number, $k_1 = 2kd/\sinh(2kd)$ the velocity correction factor, H (m) the wave height, k the wave number, $\Delta = (\frac{\rho}{\rho_w} - 1)$ the buoyant density of the GSC, ρ (kg/m^3) the mass density of the GSC, l (m) the length of the GSC, W (N) the weight of the GSC, k_w the GSC volume factor ($k_w = V/l^3$), γ (N/m^3) the GSC specific weight, and V (m^3) the volume of the GSC. The author then established 4 damage levels, in an analogy to the damage levels of De Vos et al. (2012) – no movement (Damage 0), small movement of the GSCs closest to the monopile (Damage 1), relevant movement of GSCs in the protection's total area (Damage 2), large number of GSCs closest to the monopile removed (Damage 3/Failure). By analysing the values obtained for N_s^*, and by comparing them to the visual damage levels defined, Corvaro et al. (2018) reported that GSCs are stable for $N_s^* < 1.2$, which corresponds to the Damage 0. Supposing that larger damage levels could be obtained, it suggested that an acceptable $N_s \times$ value for the design of GSCs characteristics (W and/or l) could be 1.5 – value corresponding to Damage 1. Wang et al. (2023a) also tested circle and square-shaped mattresses for monopiles. Mild scour damage was detected at the corners of the squared configuration. However, despite the effective behaviour that the geotextile appears to have on scour, Wang et al. (2023a) also highlights potential negative impacts on the marine environment and species;

- **Microbially Induced Calcium-Carbonate Precipitation (MICP) and Ionic Soil Stabilizers (ISS):** these relatively new and eco-friendly techniques are based on biological processes for soil improvement. It involves the formation of calcium carbonate ($CaCO_3$), for MICP solutions, or the mixture of cations Ca^{2+}, Mg^{2+}, and Na^+, with anions NO_3^- and SO_4^{2-}, for ISS solutions, by forming a binder with the soil sediments, thus increasing strength and the seabed's resistance to scour (Zhang et al., 2023). According to Li et al. (2022b), MICP has been used for soil stabilization for over two decades. Li et al. (2022a) used MICP to investigate the wave erosion resistance of sandy slopes. The results showed that after two MICP treatments, the resistance of the slope was not improved, as the cementation solution permeated into the bottom. However, after four treatments, the slope's permeability decreased, the cementation remained on the top layer of the slope, and the topography remained unaffected by the wave conditions. So, as a scour protection around a monopile, Li et al. (2022b) used this method to assess its resistance under current-only conditions (Fig. 6d). It concluded that the maximum S/D was reduced up to 84% after only two treatments. When using four treatments, no scour was detected in the vicinity of the foundation, as the calcium carbonate crystals increased the cohesion and coating of the sediment particles. It also noted that, as scour decreased due to the cementation effect, depositions at the downstream side of the foundation disappeared but edge scour depth/length increased. The author reflects on the necessity to reflect and consider a balance between MICP protection and edge scour. Moreover, it proposed an equation that relates the S/D and the protective strength ratio (R) – quotient between the penetration resistance of the MICP-protected position and the unprotected position:

$$S/D = 0.055 + 1.62 \times 0.67^R \tag{6}$$

As for ISS solutions, they are usually applied for silts, silty clays, or sandy silt soils, forming a solidified slurry. Hu et al. (2022a) compared the scour of an unprotected monopile to a monopile with an ISS scour protection under currents-only and combined waves and currents. The ISS was applied with a dispersion resistance agent, silt, and distilled water (3 different mixture ratios). The results showed that the use of ISS was extremely efficient by enhancing the soil's critical shear stress, leading to a reduction of the relative scour depth (S/D) in the range of 90%–95% when compared to the unprotected monopile. Hu et al. (2022a) also points out the fact that scour evolution curves plotted for the cases when ISS was used, showed less fluctuation and a smaller value for the time scale period of the scour process (T_c). That was pointed out as an indicator that fewer ripples emerged around the foundation, that the equilibrium scour is achieved faster, and that the incipient motion of the sediments could be more difficult under the same hydrodynamic conditions. Hu et al. (2022b) used a similar approach to assess scour in a pipeline under regular waves and combined waves and currents. The results also show that ISS could prevent scour by decreasing the soil porosity and by enhancing the necessary critical shear stress for initial sediment motion. Overall, a S/D reduction between 70% to almost 100%, in some cases, was obtained when comparing a protected to an unprotected pipeline. However, Hu et al. (2022b) highlights two potential problems. The use of ISSs on soils where a non-cohesive layer exists underneath the solidified ISS layer could result in accumulated liquefaction as the solidified layer will prevent the dissipation of pore pressure. Besides, it also mentions that pouring ISS-solidified slurries in scour pits in the ocean environment could damage the habitats of benthic fauna that need soft soil to hide from predators.

- **Artificial Reefs (AR):** this scour protection has previously been demonstrated to effectively reduce wave-current energy, block sediments, and prevent erosion on shorelines or when combined with breakwaters while increasing biodiversity (Srisuwan and Rattanamanee, 2015; López et al., 2016; Marin-Diaz et al., 2021; Kim et al., 2021, 2022). However, relative to their use and performance in OWT foundations, Zhao et al. (2023) concluded that there is a lack of research on the topic. Therefore, a 3D numerical model was built by Zhao et al. (2023) to study the effect of ARs on flow characteristics and scour under steady flow around an OWT. Multiple arrangements were used to assess and compare the best spacing, the best protection performance, and the best efficiency for maximum scour depth. Based on the results, it was possible to conclude that ARs reduce scour by 20%–30%, depending on the arrangement (single, parallel, tandem or stack ARs) and distance from the OWT foundation. Aleksandrova et al. (2023) performed large-scale wave-only tests (scale factor 1:6) and small-scale wave-current tests (scale factor 1:30) on multiple eco-friendly scour protection layouts for monopiles (Fig. 6e) and cables (Fig. 6f), by integrating artificial reefs (reef balls and holey pipes), oysters and loose shells on a double-graded riprap scour protection. The aim was to assess the effect of edge scour on the stability of those eco-friendly elements. The test results have shown that the AR structures when compared to a control case (monopile only with scour protection), did not induce extra deformations. The deformation pattern is shifted depending on the placement of the structures. Therefore, ARs may have some influence on the deformation patterns. Moreover, they tend to become unstable under severe hydrodynamic loading, mainly when placed inside the monopile amplification zone (radius equal to 3 times the pile diameter). That may cause collisions and damage to the surrounding infrastructure. Aleksandrova et al. (2023) highlights the importance of avoiding areas of the scour protection where significant flow amplifications and large reshaping of the armour layer may occur. For the holey pipes, no significative displacement was registered when embedded inside the armour layer even in the amplification zone, unlike when placed on top of the filter layer where larger displacements were registered even under milder conditions. The

pipes also have shown some potential for sediment depositions and infills. Hence, these results point out the importance of accounting for the hydrodynamic shape, the submerged weight of the structures, the embedment into the protection layers, and the possible requirement of an anchoring system to keep stability while maintaining the ecological benefits. Nonetheless, the sediment infill can compromise the sheltering effect for biota and substrate species. Finally, regarding the stability of loose oysters and shells for cable protection, they have shown good behaviour in small hydrodynamic conditions. Significant displacements only started to appear for intermediate conditions. Nonetheless, no detrimental effects for the scour protection below were registered, highlighting the limited risk of this concept when compared to the installation of larger AR structures. Overall, as a scour protection ARs can have a positive effect on reducing turbulence on the foundations, depending on their placement.

Other alternative countermeasures, such as bionic grass (a low-maintenance fibre mat composed of several artificial grasses) and honeycomb protection (multi-compartment structure used in shoreline protection to improve growth of vegetation and restrict sediments motion), Fig. 7, have also showed the capacity to decrease scour depths and enhance sediment depositions, Schendel et al. (2014).

Although alternative scour protection studies are gaining increasing momentum, they usually do not consider or quantify other important factors such as cost, adaptability, reliability, impact on biodiversity, marine environment pollution, and greenhouse gas emissions at the production level. However, a multi-criteria comparison was made by Zhang et al. (2023), taking into account factors such as adaptability, cost, environmental impact, concerns with the armour layer, soil improvement, pile attachment, seabed attachment, and biological protection for the most recent research findings in the literature. The conclusions extracted by Zhang et al. (2023) were that armouring layer protections (riprap and geotextiles), soil improvement techniques (MICP and ISS), and biological protections (bionic grass and ARs) had a higher overall score compared to active protection systems such as collars, vanes, and sacrificial piles active. Conversely, Zhang et al. (2023) points out the lack of practical application cases for soil improvement and biological protections. Moreover, Zhang et al. (2023) mentions that limited to no research has been performed on the impact of scour countermeasures on the marine environment, thus stressing that further
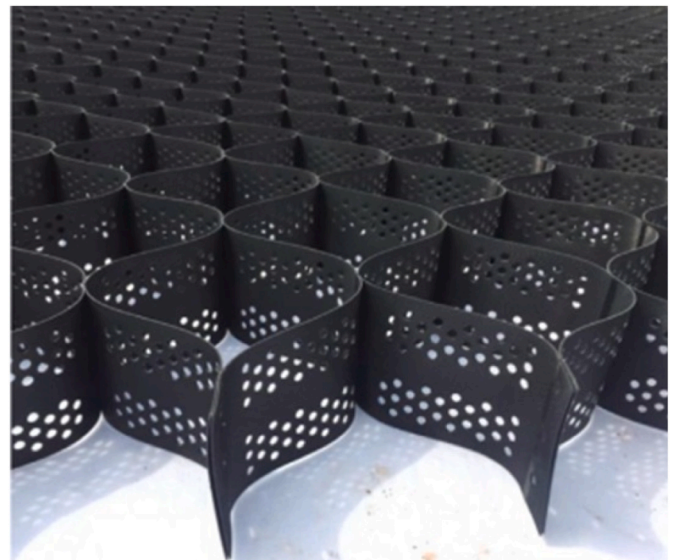

Fig. 7. - Honeycomb scour protection – Reprinted with permission from Wang et al. (2023a), Copyright 2023, Elsevier.

research should be made for a more comprehensive comparison.

In the end, both scour protection optimization and eco-friendly scour protection studies are crucial, as scour is a structural and financial risk and no design equations have been yet proposed or can be found in the literature, mainly for complex and hybrid bottom-fixed foundations. Typical solutions such as riprap protections have been proven to perform at a very high level in multiple engineering applications. It is now necessary to determine if the existing design formulas for monopiles are transferable and viable for other types of offshore foundations, or even if it is necessary, to improve them – to enhance cost reductions or improve savings of different in situ solutions when compared to the static protection concept. The following chapters will focus on scour and scour protection studies performed in complex and hybrid bottom-fixed foundations.

3. Scour and scour protections at complex foundations

In recent years, the focus of research related to marine renewables' energy has been looking to the possibility of co-located harvesting technologies, which require the development of hybrid foundations, i.e., a foundation where more than one technology can be installed. Given the possibility of risk and investment sharing among technologies that are simultaneously exploited, hybrid foundations represent a field of research with growing potential. The co-location of OWTs, WECs, TECs, and other technologies, often implies the use of marine foundations with complex geometries, that present scour behaviour that is rather different from the one presented by monopiles (Fazeres-Ferradosa et al., 2021).

Scour on complex bottom-fixed foundations, with complex geometries and features, has been increasingly discussed in recent years (Fazeres-Ferradosa et al., 2021). However, scour protections for these complex foundations are still a topic not fully addressed. With the application of energy converters, problems directly or indirectly connected to scour, such as instability, fatigue, or differential settlements, could be enhanced or diminished, thus directly affecting the protection behaviour.

The existing scour prediction and design formulas, and other scour countermeasures, were developed mainly for monopiles. Yet, for complex structures, those approaches are usually conservative and some methodologies do not translate directly, since they do not account for the foundations' different shapes or even for the increased importance of local scour (Fazeres-Ferradosa et al., 2021).

To better comprehend the basis of the scour on complex foundations and the structure features' influence on scour mechanisms, it is extremely important to understand scour around pile groups first. For wave-induced conditions, scour depths around pile groups not only increased with increasing Keulegan-Carpenter numbers (KC) and pile diameter (D_p), but was also highly reliant on pile spacing G/D_p – being G [m] the gap between piles (Sumer et al., 1992). For currents, scour on the pile group surrounding areas, is primarily caused by the increased flow velocity that bursts between the piles' gaps – aggravating the turbulence generated by each individual pile (Sumer et al., 2005).

The interference that an arrangement of two or more pile groups can have on each other could be detrimental, either by placing them "side by side" or "in tandem". For piles "in tandem", the possibility of local scour holes overlapping could lead to a larger scour pit between piles. However, a sheltering effect can also occur at the downstream pile, due to the flow obstruction combined with sediment depositions (Welzel, 2021). Qi et al. (2019) presented similar conclusions when using waves and currents on tandem piles, as the horseshoe vortex on both piles loses swirling strength, thus leading to a scour depth reduction.

For piles placed "side by side", it was observed that when $G/D_p = 0$, scour depths were two times higher compared to a single pile (Beg, 2008). That difference only thinned for a $G/D_p > 6$, in line with the reports of Breusers (1972), stating that hydrodynamic interactions only start to become negligible for distances larger than $6D_p$.

These findings indicate that scour around complex foundations may be heavily reliant on additional structural elements and features. A more comprehensive description of the concepts derived from scour at pile groups to complex foundations was taken by Welzel (2021). This review seeks to summarize the most recent research carried out on scour and scour protections for bottom-fixed complex foundations.

3.1. Jackets

Jackets are structures assembled with steel tubular elements, suited for intermediate waters – heavily used on offshore oil and gas platforms. It is the second most common type of foundation used for offshore wind turbines (Fig. 3), and the most popular among complex foundations (WindEurope, 2021b).

The different structural configurations of a jacket, according to the presence of other elements, such as the diagonal bracings, horizontal elements, and J-tubes, cause a blockage effect, altering hydrodynamic conditions. This results in flow contraction, increasing current velocities, lee side vortices, turbulence, and enhances sediment transport gradients, consequently increasing scour in the vicinity of the structure (Fazeres-Ferradosa et al., 2021). Some structural characteristics like diameter, angle, and distance between braces can magnify or diminish this blockage effect (Welzel et al., 2019a). A comparison of the scour depth between two jackets with different distances of the lowest node and diagonal braces to the seabed is validated by Welzel et al. (2020). This study also concluded that even a small change of the lowest node's distance can have a significant impact on scour, i.e., lower node and diagonal braces distances to the seabed lead to deeper local erosion in the piles' vicinities and increased erosion around the footprint area for a regime dominated by currents. However, there is less global scour in conditions where waves prevail.

When some in-situ scour depths were compared to predicted values of monopile's design formulas (Welzel et al., 2019a; Bolle et al., 2012), a discrepancy between values was detected. In fact, scour depths in the field can reach considerably higher values (Bolle et al., 2012). This reinforces the idea that more studies are still necessary to develop more accurate predictive formulas (Fazeres-Ferradosa et al., 2021).

Novel empirical expressions (Equation (7a)), based on the approach of Welzel et al. (2019a), account for the influence that the distance of both the node and the inferior diagonal brace nearest to the seabed can have on scour (Welzel et al., 2020) – where U_{cw} is the wave-current velocity ratio, and coefficient B is included to distinguish the impact of the distance to the seabed of the lowest node (Fig. 8). Parameter A differentiates the upstream (A_{front}) and the downstream (A_{rear}) sides of the structure. It is also a reference distance times the structure footprint length (Fig. 9), i.e., to estimate scour at the footprint 1.0A should be used, to estimate scour at an area of influence equal to two times the footprint 2.0A should be used, and so on.

As shown in Table 2, overall the S/D values tend to be higher for pile 1 (pile further ahead facing both waves and currents) than pile 3 (pile further back facing both waves and currents), indicating that the most exposed pile to hydrodynamic conditions has the most necessity to be protected. It also indicates that the relative scour depth tends to increase for higher values of U_{cw} for the same value of KC, showing that scour aggravates for increased hydrodynamic conditions mainly for current dominated conditions ($U_{cw} \geq 0.5$).

$$\frac{S}{D} = \left(0.7 + exp\left(-6.5U_{cw}^{2.5} - A\right)\right)^{1.5} + B \tag{7a}$$

with

$$A_{front} = 1.66KC^{0.34} - 4.5 \tag{7b}$$

$$A_{rear} = 1.30KC^{0.40} - 4.6 \tag{7c}$$

$$B = \begin{cases} 0.17, \, node \, distance = 0D \\ 0.22, \, node \, distance = 1D \end{cases} \tag{7d}$$
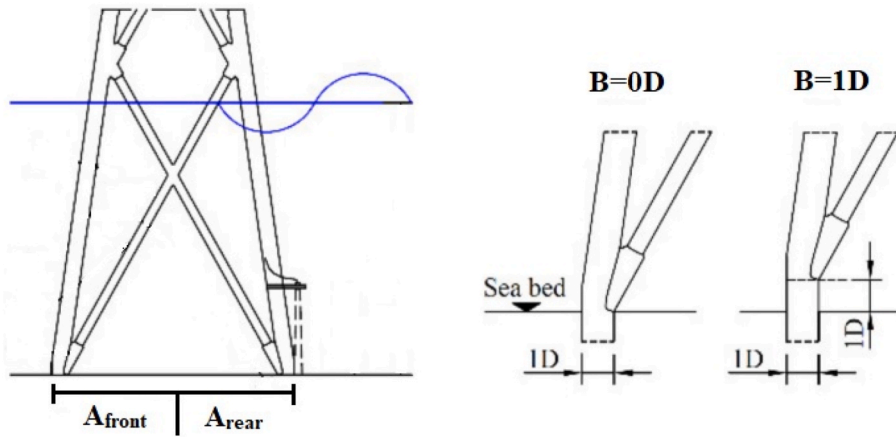
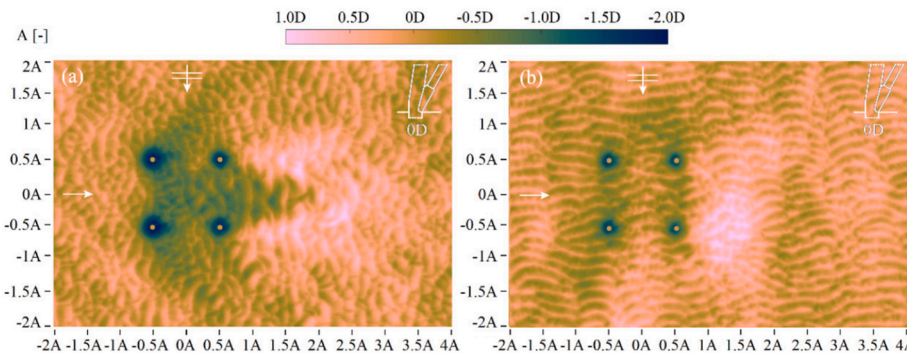**Fig. 8.** - Visual representation of the parameters *A* and *B* – adapted from Welzel et al. (2020).

Fig. 9. Surface elevation for scour tests (node distance: 0D), over a distance A to the centre of the foundation (blue and green: scour, brown and pink: sediment deposition), for: a) $KC = 6.7$ $U_{cw} = 0.75$; b) $KC = 14.9$ $U_{cw} = 0.56$ – adapted from Welzel et al. (2020).

Table 2
- Test results and conditions for jacket scour tests (Welzel et al., 2020) – prototype values.

Test	Node Distance (m)	Hs (m)	Tp (s)	Um (m/s)	Uc (m/s)	Ucw (−)	Wave-Current Direction	KC (−)	S/Dpile1 (Front)	S/Dpile3 (Rear)
1	0D	4.41	10.95	0.73	0.55	0.43	90°	6.7	0.403	0.238
2					1.23	0.63			0.801	0.786
3					2.13	0.75			1.571	1.268
4		4.74	18.62	0.96	0.55	0.37		14.9	0.884	0.580
5					1.23	0.56			1.317	1.075
1	1D	4.41	10.95	0.73	0.55	0.43	90°	6.7	0.464	0.271
2					1.23	0.63			0.863	0.708
3					2.13	0.75			1.502	1.133
4		4.74	18.62	0.96	0.55	0.37		14.9	0.735	0.622
5					1.23	0.56			1.205	1.038

Also, new volume analysing methods, as well as dimensionless parameters were provided, capable of being adapted for offshore complex foundations (Welzel et al., 2019b). It also includes the derivation of equations to predict maximum erosion volumes (Equation (8)) and cumulative erosion volumes (Equation (9a)), over a certain distance *A* to the centre of the structure. The tests revealed that the area of the seabed affected by the structure is considerably larger (between 2.1 and 2.7 times the structure's footprint), where the maximum erosion intensity appears to be found in the vicinity of an area equal to 1.25 times the structure's footprint area.

Global and local scour give different indications of scour patterns around the structure. Local scour indicates that the scour holes develop mainly around the foundation piles, whereas global scour indicates that the scour rate and depth are extended around the entire jacket foundation (Welzel et al., 2019b). A comparison between local and global erosion volumes revealed that, for wave-dominated conditions, scour depth and patterns are dominated by local scour (68%), opposite to current-dominated conditions, mainly for $U_{cw} \geq 0.75$, where scour depth and patterns are governed by global scour (67%), (Welzel et al., 2019b). These values indicate that for zones where hydrodynamic conditions are dominated by waves, scour protections should be designed only for each pile or reinforced with a higher thickness near the piles, whereas for current-dominated zones, scour protections should be reinforced near the piles but also designed for a much higher extent, to cover the structure's footprint area and the surroundings.

Although both studies do not consider scour protections, they could be helpful to develop them. They provide valuable information about scour patterns (Fig. 9), scour depth (Table 2), and erosion volumes, indicating the extent, thickness, and where the scour protection should be reinforced. Moreover, the results when compared to in situ data (Bolle et al., 2012; Baelus et al., 2018; Rudolph et al., 2004) showed good correspondence (Welzel et al., 2019b).

$$V_{A,max} = -1.3(0.1 + exp(-4.6U_{cw}))^{1.5} \tag{8}$$

$$V_{A,i} = V_{Area} - 1.3(0.1 + exp(-4.6U_{cw}))^{1.5} \tag{9a}$$

with

$$V_{Area} = \begin{cases} ((0.1 + \exp(-10A + 8))^{-0.9}B' - C', A < 1.25A \\ -2.2\exp(-0.7A) - 0.11, A > 1.25A \end{cases} \tag{9b}$$

$$B' = (-5.2U_{cw} + 6.9)10^{-2} \tag{9c}$$

$$C' = (3.8U_{cw} + 4.9)10^{-1} \tag{9d}$$

Recently, Welzel et al. (2024) performed a comparative study of a novel complex foundation to a standard 4-legged jacket, under unidirectional currents in clear-water and live-bed conditions. The description and results of the novel foundation are reported on Chapter 3.5. Regarding the jacket foundation, Welzel et al. (2024) reported that for clear-water regime no global scour was observed, being apparent that the foundation's structural elements and features have a small influence on the scour process. It was observed that local scour holes increase faster at the upstream piles that shelter the downstream piles. During live-bed conditions, the foundation showed the presence of global scour since erosion was detected around the piles and in centre of the foundation. Nonetheless, global scour progressed slower than local scour. Moreover, sediments began to accumulate downstream of the structure. When compared to the results of combined wave-current conditions of Welzel et al. (2019a), the scour development observed by Welzel et al. (2024) shows higher disparities in the local scour development between the upstream and downstream piles. Welzel et al. (2024) also compared its results to in-situ field data, verifying a good agreement of the erosion spatial distribution and mean dimensionless scour depths.

Some of the observations under clear-water regime reported by Welzel et al. (2024) are corroborated by the experimental campaign performed by Chen et al. (2023) on 4-legged jacket under unidirectional currents. Chen et al. (2023) tested different flow directions (by rotating the foundation), different water depths, different flow strengths (ratio between the current-averaged velocity and the critical velocity of sediments), and in the end performed a result comparison to a monopile. The major conclusions are outlined below.

- For a 0° foundation angle (two piles facing currents), maximum scour depths occur at the front piles. The back piles due to a sheltering effect and due to the eroded sediments from the front piles, registered lower scour depths;
- For a 45° foundation angle (one pile facing currents), the maximum scour depths occur at the middle row of piles, as the flow behind the front pile increases and the change on the position of the upper truss enhances turbulence;
- Variations on the foundation angle reduce the sheltering effect of the front pile(s), as the remain piles begin to be directly affected by the incoming hydrodynamic conditions and the reduction of the distance between the front piles increase the jet flow effect;
- Maximum scour depth in directly related to the flow strength and water depth if the remaining conditions are kept constant. Moreover, the time for scour to reach a quasi-equilibrium stage increases with increasing flow strength;
- The scour process on a monopile tends to be slower and the maximum scour depth and extent are lower when compared to a jacket foundation, indicating that the structural elements and features have a strong influence;

Numerical models were also performed to compare predictive values with in-situ measurements. Numerical simulations of the C-power wind farm Thornton Bank, under currents and waves, were carried out to predict local scour (Ahmad et al., 2020). The results of maximum scour agreed well with the reports for a 4-pile jacket foundation (Bolle et al.,

2012). A numerical model of a multi-bucket jacket foundation that resulted in the suggestion of a scour prediction formula for currents based on dimensionless parameters for a certain range of values (Table 3) was also developed (Lian et al., 2022).

Few recent works tested scour protections for jacket foundations. An extensive review of those works can be found in Fazeres-Ferradosa et al. (2021).

Table A.1 gives a brief overview of some physical model tests. The main conclusions of those studies are as follows.

- An East Anglia One offshore wind farm 3-legged jacket foundation model (Fig. 10), with front mats and high-density rip rap scour protections, has been tested for three cumulative sequential tests of waves and currents (ascending, descending, and random), Sarmiento et al. (2021). The erosion patterns were similar for all sets of tests. It was concluded that a decreasing sea state sequence leads to larger erosion and cumulative damage when compared to an increasing or random sequence. For the most exposed jacket leg, a maximum scour depth equal to $5D_{50}$ was registered for the descending sequence. As for the ascending and random sequence, the maximum scour depth value obtained was equal to $3D_{50}$. The least exposed jacket leg registered a maximum scour depth of $2D_{50}$ for the least favourable sequence of tests. Regarding the scour extent, the worst case was also recorded for the descending sequence, over the ascending or random sequence (approximately 0.5*D* from the edge of the jacket leg);
- Jacket foundation models' of the HZK Offshore Wind Farm and the Borssele Wind Farm and OHVS (Fig. 11), respectively, with different displacements of the material of the scour protection have been tested (Van Velzen et al., 2016; Van Velzen and Bruinsma, 2017; Bruinsma et al., 2018). Three different configurations of the scour protections were studied: a single layer with a post-installed jacket and a two-layer system with a post- and pre-installed jacket. Results showed some similarities between both studies and concluded that the scour protection was quite stable, either applied pre- or post-installed jacket. The two-layer system, with the armour layer placed after the jacket's installation, was deemed the worst option regarding the armour layer stability. The study also highlights the importance of the filter layer in a two-layer protection system;
- A 4-layer scour protection around a jacket foundation model for waves and currents (Fig. 12), as well as an alternative, soft scour countermeasure, i.e., coastal cage net for aquaculture was tested (Hsin-Hung et al., 2014). Both solutions proved to be effective and resulted in a reduction of the scour depth. Moreover, the integration of a coastal cage net shows that it can be meaningful and helpful to prevent scour around offshore foundations;

While there is a clear lack of studies on scour protections applied to jackets, in recent years, the number of scour model tests performed on jackets has been increasing for both physical models (Welzel et al., 2019a, 2019b, 2020; Hsin-Hung et al., 2014) and numerical models (Ahmad et al., 2020; Lian et al., 2022). They aim to cover important parameters such as the relative scour depth (*S/D*), the scour width, the dimensionless time scale (*T**), the equilibrium scour depth (S_{eq}), eroded

Table 3
– Numerical model conditions by Lian et al. (2022).

Reference	Lian et al. (2022)
d (m)	40
U_c (m/s)	1
U_{max} vortices (m/s)	[1.35–2.76]
Calculation time (s)	3600
Output time (s)	300
Bucket Diameter (m)	[10–30]
Bucket Spacing (m)	[30–50]
Bucket Exposed Height (m)	[0–3]
Hydrodynamic Load	Currents only

Fig. 10. - Scour protection for a model of the East Anglia One 3-leg jacket (Sarmiento et al., 2021).

Fig. 12. - Scour protection model for a 4-leg jacket (Hsin-Hung et al., 2014).

3.2. Tripod foundations

Tripods are complex structures composed of three piles connected to the main column by diagonal braces, best suited for intermediate waters. Studies involving scour protections for this type of complex structure are not common. The scour process and its development for tripods are quite different from monopiles or even from sets of piles.

Tests with tripods, hexapods, a triangular array of circular cylinders (TACC), and a hexagonal array of circular cylinders (HACC), have been performed under currents, and compared to each other and monopiles (Ni and Xue, 2020). The work shows that the relative maximum scour depth (S_{end}/D) is approximately 30% higher for tripods and hexapods than for TACCs and HACCs, respectively, proving that the lower diagonal braces of the complex structure cause blockage effects, enhancing scour phenomena.

A setup of physical and numerical model tests to assess scour on tripods under regular waves (scale: 1:40, $H = 8.25$ m, $T_m = 19$ s, and $d = 30$ m – prototype values) was performed for a 4000-wave cycle. Scour was observed under the main column, around the lower braces connecting the piles to the columns, and at the front/rear piles. For the physical model, the rear piles registered the highest relative scour depth ($S/D_{pile} = 0.85$). As for the front pile, S/D_{pile} decreased to 0.59, and under the main column, S/D_{column} was equal to 0.44. Scour under the main column and the lower braces can be explained due to the blockage effects mentioned in Ni and Xue (2020). Scour depths were in an almost equilibrium stage after 3000 waves, with 90% of the corresponding values reached after 1500 waves. The scour patterns identified were similar to other researchers' findings (Stahlmann and Schlurmann, 2010; Harris and Whitehouse, 2014). Regarding the numerical model, for the front pile, scour depths were in good agreement with the experimental results. However, scour depths at the rear pile and under the main column were about 20% lower and 32% higher, respectively. This difference had not a clear explanation, and it was assumed to be related to hydrodynamic processes and wave absorption procedures.

The research comparison between in-situ data (*Alpha Ventus* Offshore wind farm), large-scale (1:12), and small-scale (1:40) tests performed by Stahlmann and Schlurmann (2010) allows to extract similar but further conclusions from those in Stahlmann (2014). The tests were performed for regular and irregular wave cycles, for different incoming wave angles (Fig. 13): 0° - one pile facing waves, 30° - asymmetric constellation, and 60° two piles facing waves. Table A2 gives a brief overview of the setup conditions, some of the S/D values obtained for the 0° configuration under regular waves with maximum wave height and period, and the in-situ measurements.

Overall, both the large- and small-scale tests allowed to state that global scour (highly related to scour extent) and local scour (highly
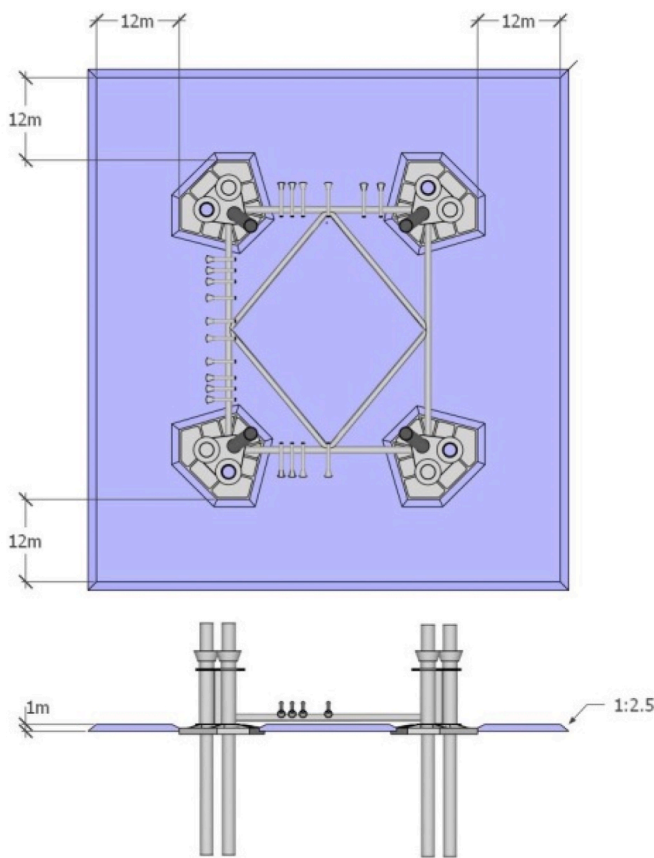

Fig. 11. – Scour protection layout for a 4-leg jacket model of the Borssele Offshore High Voltage Station (Bruinsma et al., 2018).

volumes and areas, and scour estimations when a regime is dominated by currents, by waves or equally dominated. One of the reasons is that there has been a growing interest in reusing old platforms to install OWTs, but also in using jackets for offshore high-voltage stations. In addition, there has been an increased effort to develop scour design equations since monopile's formulas predict inaccurately the phenomena for complex structures. New findings can serve as a base and lead to further studies to develop novel dynamic design formulas for scour protections.
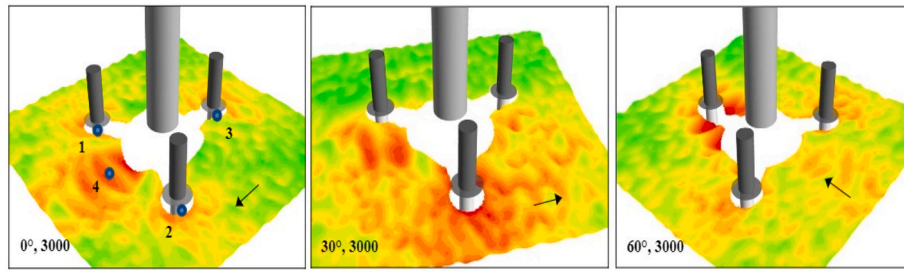
Fig. 13. – Scour development for different incoming wave angles – adapted from Stahlmann and Schlurmann (2010).

related to scour depth) were very dependent on the wave direction. Comparing the results between both scale tests, it was worth noticing that the 1:12 tests obtained S/D values for the structural elements almost 50% higher than the small-scale tests. As for the near field of the structure, the difference was explained by the influence of the ripple formation. The large-scale tests also showed that regular wave conditions, with wave heights and periods similar to irregular wave conditions, led to higher sediment mobility around the structure, increasing global scour – despite local scour at the piles and under the main column reaching similar values (Stahlmann and Schlurmann, 2010). Regarding the in-situ measurements, when compared directly to the large-scale tests, the registered *S/D* values were larger, mainly under the main column. These differences were attributed to the tested model wave conditions (real sea state conditions and wave directions were simplified), scale effects of the sediments (not properly scaled to maintain non-cohesive properties), and mainly the fact that only waves were used, instead of real wave-currents offshore conditions (Stahlmann and Schlurmann, 2010). However, both models had a good agreement with the in-situ measurements regarding the development and extent of local and global scour – maximum scour depths and shapes occur at similar spots.

For tests under currents and waves, a tripod with 3 different orientations was studied (Hu et al., 2021), according to the position of the wave-current direction: (i) 0° - a pile facing the wave-current direction; (ii) 90° - asymmetric, with the wave-current direction being perpendicular to a brace; and (iii) 180° - two piles facing the wave-current direction. The maximum scour occurs beneath the main column, while the scour patterns extend into the area of the inferior diagonal braces as in Heibaum et al. (2010). The aforementioned blockage effect explains these characteristics, which increase the shear stress on the seabed by causing streamlined contraction (Hu et al., 2021). However, results also showed that for the 90° orientation, a higher *S/D* value was reached. The following main conclusions can also be stressed (Hu et al., 2021).

- diagonal braces facing waves and currents increase the blockage effect;
- when currents are superimposed, the dimensionless time scale for a 90° orientation increases, thus the equilibrium states are achieved for a longer time-scale;
- the comparison of experimental data with predicted values of the equilibrium scour depth formula (Sumer and Fredsøe, 2002), Equation (10a), revealed that the experimental results were on average 25% higher, for the 90° orientation. Therefore, it recommends the use of a safety coefficient of around 1.3 when using the following equation.

$$\frac{S_{eq}}{D} = (S_{currents} / D) \bullet \{1 - exp[-A^{'} \bullet (KC - B^{''})]\}; KC \geq 4 \tag{10a}$$

$$A^{'} = 0.03 + 0.75 U_{cw}^{2.6} \tag{10b}$$

$$B^{''} = 6\,exp(-4.7 U_{cw}) \tag{10c}$$

The results obtained, indicate that probably some of the current

methodologies could be adapted to predict scour and possibly to design scour protections for tripods (Hu et al., 2021). Therefore, it proposes two new equations that relate the S_{eq} with the Froude (*Fr*), Equation (11), and Euler number (*Eu*), Equation (12), for waves and currents. The results reveal that S_{eq} increases gradually and approaches an asymptotic value when *Fr* and *Eu* increase. Hu et al. (2021) considers that both formulas give a general representation of the scour depth varying trend, despite some discrepancy between the experimental data and fitting results – experimental data generally distributed within a margin of error of ±30%. In the end, it recommends that scour protections around tripods should have larger thicknesses when compared to monopiles and be reinforced in critical areas such as under the main column and diagonal braces.

$$\log\left(S_{eq} / D\right) = -0.23\exp\left(0.33 / Fr\right) + 0.49 \tag{11}$$

$$\log\left(S_{eq} / D\right) = 0.34\exp\left(-0.05 / Eu\right) - 0.16 \tag{12}$$

A numerical model for random waves was performed, Hu et al. (2022c), and compared with other experimental investigations (Sumer and Fredsøe, 2001; Schendel et al., 2020). The model proved to be capable of predicting both equilibrium and maximum scour depth with relatively satisfactory accuracy. The maximum error between the numerical results and experimental values, (Sumer and Fredsøe, 2001; Schendel et al., 2020), was less than 30% in most of the cases. Moreover, all scour patterns (Hu et al., 2022c) were similar and followed the results achieved by several studies (Stahlmann and Schlurmann, 2010; Stahlmann, 2013, 2014).

It is evident that the works found in the literature are still insufficient and solely address scour depths and inherent patterns. Studies regarding scour protections for offshore wind tripod foundations were not found by the authors. Nevertheless, the information provided about local and global scour development lays a foundation for future studies of scour protection's damage and protection design since, like other complex foundations, tripods differ considerably from monopiles in terms of scour behaviour.

3.3. Gravity-based foundations (GBFs)

Gravity-based foundations (GBF) are heavy concrete structures, suited for shallow waters, and are designed so that their self-weight withstands high overturning moments. Scour and scour protections on GBFs are less studied than in jackets or monopile foundations. The majority of studies are performed by private companies, which generally do not provide sufficient data for the public due to restricted confidential policies of the sector (Fazeres-Ferradosa et al., 2019a).

Guidelines for scour management plans, and a review of scour and protections emphasize that, in non-cylindrical GBFs, some areas are more susceptible to scour due to blockage effects around their edges (Whitehouse et al., 2011b). These observations were also noticed in a model of a STRABAG foundation – a reinforced and sand-filed concrete foundation with a cross-shaped base – subjected to physical and numerical studies (Wilms et al., 2012). As a scour protection, instead of a rubble-mound armour layer, container protection with two-layered

sand-filled geotextile was used (Fig. 14).

Scour tests performed in a large physical model, with a scale of 1:17, Wilms et al. (2012) showed that the zones more prone to scour occur at the front and back shaft, bracings, and lee corners of the hollow boxes. It was concluded that sand containers were hydraulically stable as a scour protection. The numerical model showed that the foundation's cross-shaped format caused an increment in the flow field and velocities, due to the blockage effect, enhancing the scour process (Wilms et al., 2012). The manuscript also includes a small analysis and comparison of the *S/D*, for a non-protection and protection scenario, revealing that overall scour development had a high rate between 500 and 1000 waves, which then gets reduced slightly for 2000 waves. In the cases where the protection was used, it was observed that scour depths and widths were smaller, and the major difference in the results was obtained for 5000 waves, where the *S/D* value represents almost half of the value obtained on the model without protection. Given the usage of geotextile containers as scour protection, dynamic behaviour was not examined.

An application of a dynamic scour protection to a gravity foundation to investigate scour around a model of the offshore converter DolWin Beta was studied in De Sonneville et al. (2014). The scour protection applied around the rectangular foundation did not present a uniform thickness, since a different methodology was used, i.e., the reinforcement of critical areas and the usage of a smaller thickness on sheltered zones. Dynamic stability was observed for the conditions used, even if only for 2000 waves. It was concluded that the use of stones with larger density can be used for optimization purposes since enhanced stability was achieved for reductions in volume and rock size. It also determined that currents have major importance in scour even for a wave-dominant regime.

A physical model study of dynamic scour protection for the Adriatic Liquefied Natural Gas (LNG) terminal (Fig. 15) was performed by Chen et al. (2011). The structure was composed of a gravity-based structure (GBS) and two mooring dolphins. The objective was to determine the maximum scour depth, assess if a filter layer was necessary, and evaluate the edge scour of the protection. For a 1:50 scale, four scour protection layouts were submitted to wave and current conditions (Table A3) for a 100-year return period from the project site Bora winds – result in waves from North-East to East directions – and Scirocco winds – result in waves from the South-East direction. The final design consisted of an armour layer with varying thickness, varying width, and without a filter layer. The study concluded that the scour protection sustained limited damage and that the optimized layout version had an increment of the protection thickness at the mooring dolphins, and a decreased width around the main structure. The results have shown that the sharp corners of the mooring dolphins cause significant erosion. At the main structure, scour
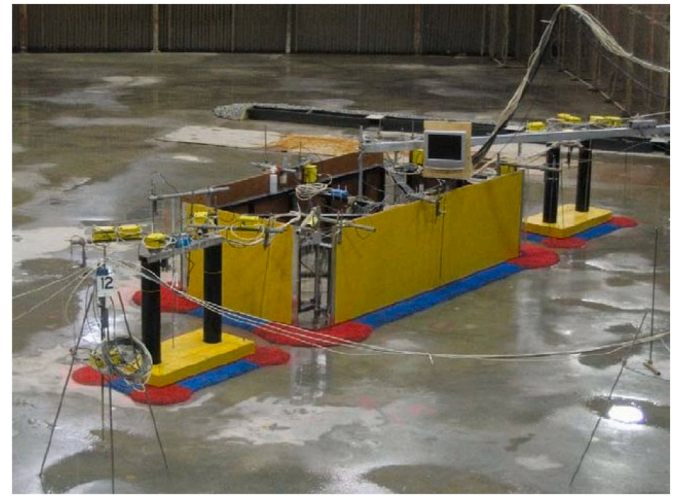

Fig. 15. - Scour protection of the Adriatica LNG terminal and mooring dolphins (Chen et al., 2011).

was also more severe in corners than around the structure's edges.

Another work regarding GBFs and scour protections provides some evidence that in a wave-dominated regime, the amplification factor of the bed shear stress is smaller than 2, Tavouktsoglou (2018). It also proposed an equilibrium scour depth formula (Equation (13a)) for complex and uniform structures, reliable for currents only but conservative for offshore conditions – where D_{base} (m) is the diameter of a non-uniform cylindrical structure, ζ is a parameter that relates the Reynolds number of the structure (Re_D), the flow depth (h [m]), the Froude number (Fr), the Euler number (Eu), the depth-averaged flow velocity (U_c [m/s]), and the mean threshold velocity of sediments (U_{cr} [m/s]), and $c1$, $c2$, $c3$ are fit coefficients. Therefore, an alternative design option based on the threshold of motion could be a future approach as stated by Fazeres-Ferradosa et al. (2021). Table A3 reports a summary of the physical models performed on scour protections for GBFs presented in the literature.

$$\frac{S}{D_{base}} = \frac{c1\zeta + c2}{\zeta + c3} \tag{13a}$$

with

$$\zeta = \left(\frac{1}{\log(Re_D)}\right)\left(\frac{h}{D_{base}}\right)(Fr)(Eu)^{0.5}\left(\frac{U_c}{U_{cr}}\right)^{0.5} \tag{13b}$$

Fig. 14. – Scour protection model of a STRABAG foundation using geotextile containers (Wilms et al., 2012).

$$c1 = [2.1, 2.3] \quad c2 = [-0.009, 0.005] \quad c3 = [0.01, 0.05] \tag{13c}$$

Gao et al. (2023) took a different approach by performing an experimental research comparison of 7 different scenarios for a 1:100 geometrically scaled GBS. The model composed of two pontoons, six supporting columns, and cross braces was tested for currents-only and waves-only conditions, for two different angles (Fig. 16): 0° and 90°. The scenarios tested compared an unprotected GBS with 6 different scour protection solutions (Fig. 18): geotextile, riprap, geotextile-riprap, bionic grass, bionic grass-geotextile, and bionic grass-geotextile-riprap. To measure scour the author used a laser scanner to extract the three-dimensional bed topographies. It was concluded that currents were the most severe hydrodynamic condition, as the relative maximum scour depth at the pontoons (S_{max}/D) of 1.12 was obtained for currents-only (90° direction) when compared to 0.193 for waves-only (90° direction), for the control scenario (no protection). When the highest U_c value was applied in the 90° direction, the platform tilted and collapsed.

By determining which was the most severe condition, Gao et al. (2023) continued the test program by implementing 6 different scour protection systems. The tests have shown that "usual" scour protections, such as riprap protections had an efficiency of reducing the scour depth of 7.0% and 55.6% when compared to the control scenario, for currents at a 0° and 90° directions respectively (Fig. 17). The geotextile-riprap, another common type of scour protection system applied in physical model tests, had an efficiency of 44.4% and 49.8%, for currents at a 0° and 90° direction respectively (Fig. 17).

The values demonstrate that the geotextile-riprap system has a more consistent performance for multiple hydrodynamic condition directions when compared to the riprap protection, with a surplus of 37.4% for the 0° direction (despite having a slightly worse performance for the 90° direction). In part, this answers some questions in the literature as to what the best filter layer material is and what are the differences in performance of the geotextile filter.

Regarding the performance of all 6 scour protections, by observing Fig. 17 it can be concluded that the bionic gras, the bionic grass-geotextile, and the bionic grass-geotextile-riprap systems were the best protection systems efficiency-wise by reducing scour in orders of 68.7% (0° direction) and of 80.1% (90° direction). The worst solution was by far the application of an only-geotextile system, with a residual efficiency for the 0° direction and a negative efficiency for the 90° direction.

Results show that perhaps the application of new and alternative materials such as bionic grass, when combined with common materials such as riprap, could be the true and ultimate optimization of scour protections. Nonetheless, to confirm the results of Gao et al. (2023), new tests with a more realistic offshore condition such as the combination of waves and currents should be applied to assess the true efficiency of the different scour protection systems used.

However, although few research studies have been made on scour protections for GBFs, the number of works is not sufficient to cover a substantial range of offshore conditions, to address or evaluate the dynamic behaviour of such protections, nor to present or optimize novel design formulas for this type of foundation. Hence, the present review highlights the importance of extending such testing conditions as a contribution to the development of scour protection design methodologies for GBFs.

3.4. High-rise structure foundations (HRSFs)

High-Rise Structure Foundation (HRSF) is a bottom-fixed structure widely used in the Asian OWS, due to the shallow depths of some Asian seas, as they represent a safe, reliable, and economical alternative (Li et al., 2017; Xiao et al., 2021; Sánchez et al., 2019). However, according to the data collected by Sánchez et al. (2019)) HRSFs have a limited optimal range of use as they only have been used until a maximum depth of 15 m and 15 km distance to the coast. It consists of a permeable foundation composed of multiple inclined piles in circular arrays that support a platform (cap), bearing high stability to axial loads, horizontal loads, and bending moments (Xiao et al., 2020, 2021; Li et al., 2017). Due to its complex layout, the flow passing through the foundation reduces the downflow and the strength of the horseshoe vortex, due to the so-called bleed flow – leading to considerable differences in the scour depth and patterns observed on monopiles (Xiao et al., 2020, 2021). Hence, equilibrium equations from monopiles tend to be conservative and overpredict scour depths at HRSFs (Xiao et al., 2021). As far as scour protections, to the authors' knowledge, there are no studies in the literature, since there have been only even a few studies covering scour for this type of foundation.

To cover some of the gaps, a comparative study between a high-rise pile foundation and a monopile was performed by Xiao et al. (2020) and by Xiao et al. (2021), using both an 8-pile and a 10-pile HRSF. The tests were performed for a scale factor of 1:50, for multiple alignment angles, and as far as the hydrodynamic conditions tested, both studies used currents-only (Table A4).

Both authors reached similar conclusions: the maximum scour depth (Fig. 19) generally occurred around the middle row of piles, $S/D_e = [0.5$ to 1.1], and was lower than the registered on the monopile, $S/D = [1.5$ to 1.7] – being D_e [m] the equivalent diameter of the foundation, *i.e.*, the diameter of a monopile which has an equal cross-sectional area to the HRSF and d_p [m] the diameter of each HRSF individual pile (Equation (14)). For monopiles, $D_e = D_p$. This was credited in part to the structural permeability, the sheltering effect of the upstream and middle piles, and the bleed-effect of the foundation. Xiao et al. (2020) observed that a higher single dune of sediment depositions occurred closer to the high-rise pile foundation when compared to two smaller dunes appearing further away from the monopile (Fig. 19). This feature was attributed to the fact that the HRSF piles decrease the sediment transport capacity of the penetrating flow. As far as the scour shape of the global scour hole, it has a serrated shape, opposite to a smooth circular profile of the monopile. The radial distance of the scour hole increases in the
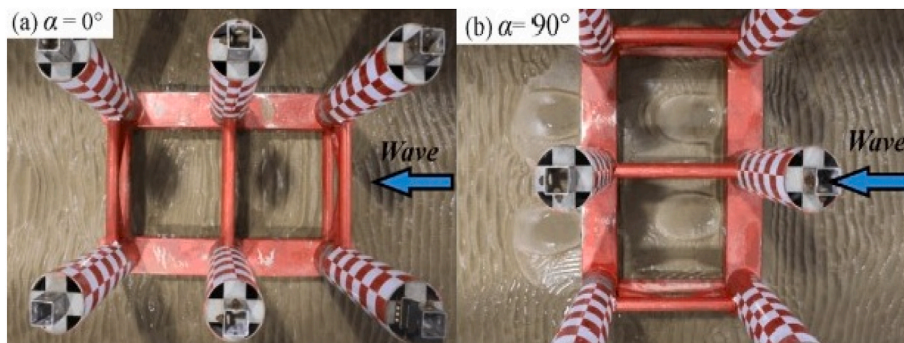

Fig. 16. - GBS submitted to waves-only for: (a) 0° direction and (b) 90° direction – Reprinted with permission from Gao et al. (2023), Copyright 2023, Elsevier.
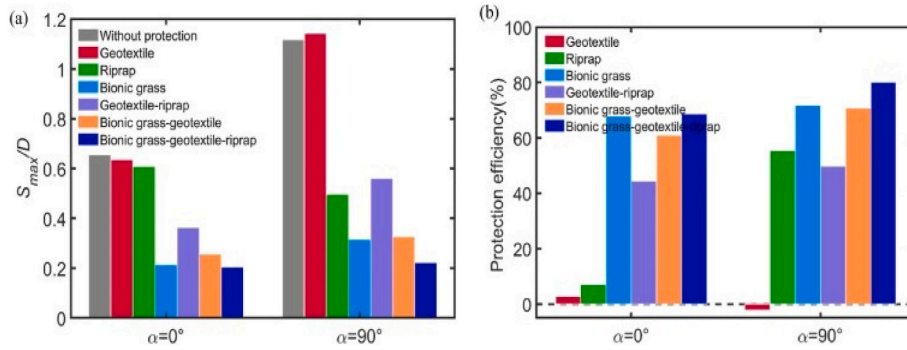
Fig. 17. - S_{max}/D and Protection Efficiency (%) for different scour protection systems for the maximum flow velocity ($U_c = 0.25$ m/s), Reprinted with permission from Gao et al. (2023), Copyright 2023, Elsevier.
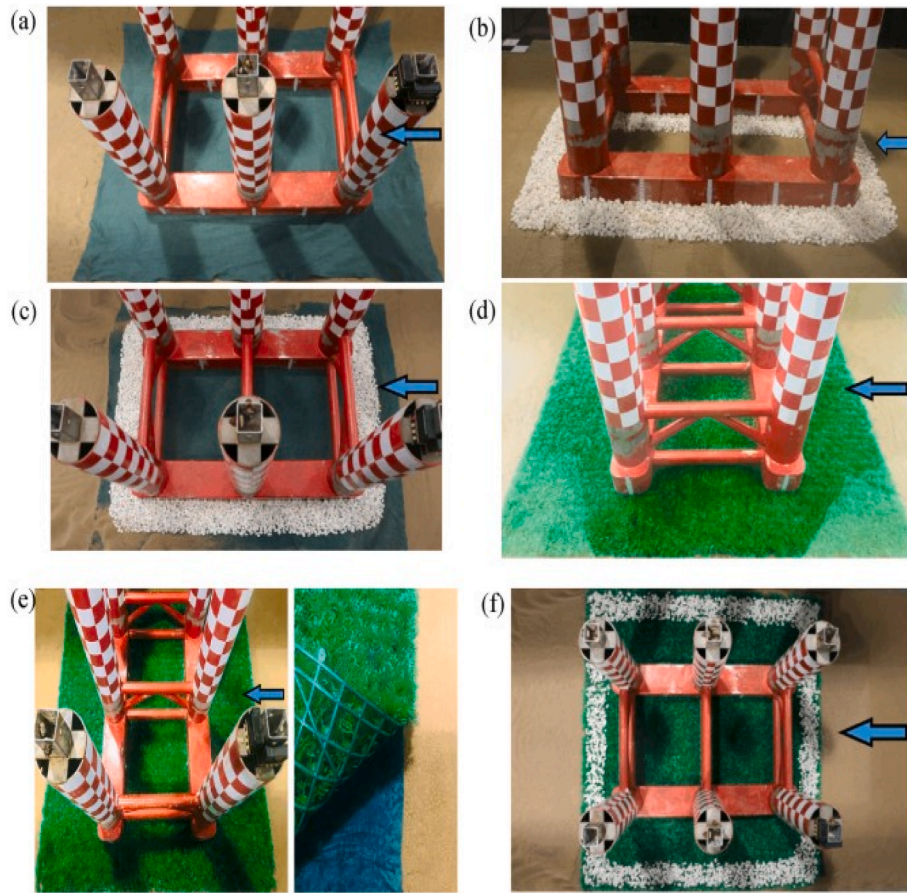

Fig. 18. – GBS scour protection systems: (a) geotextile; (b) riprap; (c) geotextile-riprap; (d) bionic grass; (e) bionic-grass-geotextile; (f) bionic grass-geotextile-riprap – Reprinted with the permission from Gao et al. (2023), Copyright 2023, Elsevier.

flow direction, changing from $1.36D_e$ (upstream) to $2.35D_e$ (downstream). Compared to the radial distance of the monopile ($2D_p$ to $4D_p$), it is possible to conclude that scour occurs much closer to the vicinity of HRSF.

$$D_e = \sqrt{nd_p} \qquad (14)$$

With the results obtained, Xiao et al. (2020) proposed a formula to predict scour radial distance (Equation (15)) and the equilibrium scour volume (Equation (16)) that can be useful for designing the minimum area of a scour protection armour layer.

$$\frac{R'}{D_e} = k' \frac{d_s}{D_e} \qquad (15)$$

$$\frac{V_s}{V_{se}} = 1 - \exp\left[-1.29\left(\frac{t}{T_e}\right)^{0.46}\right] \qquad (16)$$

being R' [m] the radial distance of scour (horizontal distance from the outer edge of the exposed piles, d_s [m] the local scour depth at an individual HRSF pile, k' [-] the constant to define the upstream (1.57), the side (1.87), and the downstream location (2.99) of the foundation, V_s [m³] the scour volume, V_{se} [m³] the equilibrium scour volume, t [s] the scour time step, and T_e [s] the scour time scale.

Table 4

Field measurements for the Dogger Bank and Horns Rev II suction bucket foundations - adapted from Stroescu (2018).

Reference	Dogger Bank East	Dogger Bank West	Horns Rev II
d (m)	25	23	20
$D_{caisson}$ (m)	15	15	12
10-year Return Period: Wave height (m)	9.1	9.8	8.1
10-year Return Period: Wave period (s)	16	15	12
Flow velocity (m/s)	1.0	1.0	[1.5–2]
θ_{cr} [-]	0.074	0.074	0.030
τ_{cr} [MPa]	0.161	0.161	0.224
Installation time (h)	6	7.5	8
Equilibrium scour depth (m)	[0.5–0.8]	[0.5–1.4]	[0.4–0.9]
Max scour depth (m)	1.5	1.9	2.0
$S_{max}/D_{caisson}$	0.1	0.126	0.166

Xiao et al. (2021) concluded that the alignment angle of the foundation facing the hydrodynamic conditions, had a negligible effect on the scour rate and the equilibrium scour depth. It proposed an empirical formula for estimating the equilibrium scour depth (Equation (17)).

$$\frac{d_{se}}{D_e} = 3.08 \left(\frac{d}{D_e}\right)^{0.40} \left(\frac{U_c}{V_c}\right)^{5.18} \left(\frac{D_e}{D_{50}}\right)^{-0.14} \tag{17}$$

being d_{se} [m] the equilibrium scour depth for HRSF individual piles and V_c [m/s] the threshold sediment motion velocity.

According to the author, this equation cannot be applied when U_c/V_c

< 0.75. However, it showed a good agreement with the available data, having the smallest root mean squared and mean absolute error when compared to existing empirical equations for monopiles. Almost all the prediction values were within the ±20% error lines, way lower than the ±50% error lines of the comparable equations.

Liang et al. (2021) also performed a series of small-scale tests to assess the characteristics of the turbulent flow fields around a 10-pile HRSF, (Table A4). It concluded that the first and second rows of piles cause an increase in the flow velocity, reaching its maximum value at the third (middle) row of piles. For small Reynolds numbers, the wake vortices could not fully be developed on the leeward side of the last row of piles – contrasting to what occurs in monopiles. The strong flow velocities and turbulence around the middle row, lead to severe scour depths around this area, to the occurrence of a long-tail pattern downstream of the foundation shoulders, and a trapezoidal deposition of seabed sediments behind the HRSF. These findings are supported by the observations of Xiao et al. (2020, 2021).

A similar study was conducted by Yagci et al. (2017), where clear-water scour was analysed for an array of circular piles, one central cylinder surrounded by other six cylinders at the vertices of a regular hexagon. Different configurations regarding the flow direction alignment and solid volume fractions (i.e., placement density of the piles) were used to determine the effects of permeability, blockage effects, and angle of attack of the flow. When comparing the results to a singular pile with an equal cross-sectional area, overall, the arrays could generate 22% less scour depth and 27% less scour volume. As stated by Yagci et al. (2017), the cross-sectional area of the array may impact the temporal development of scour. However, scour depth increment is influenced mainly by the orientation and placement density of the piles, as a
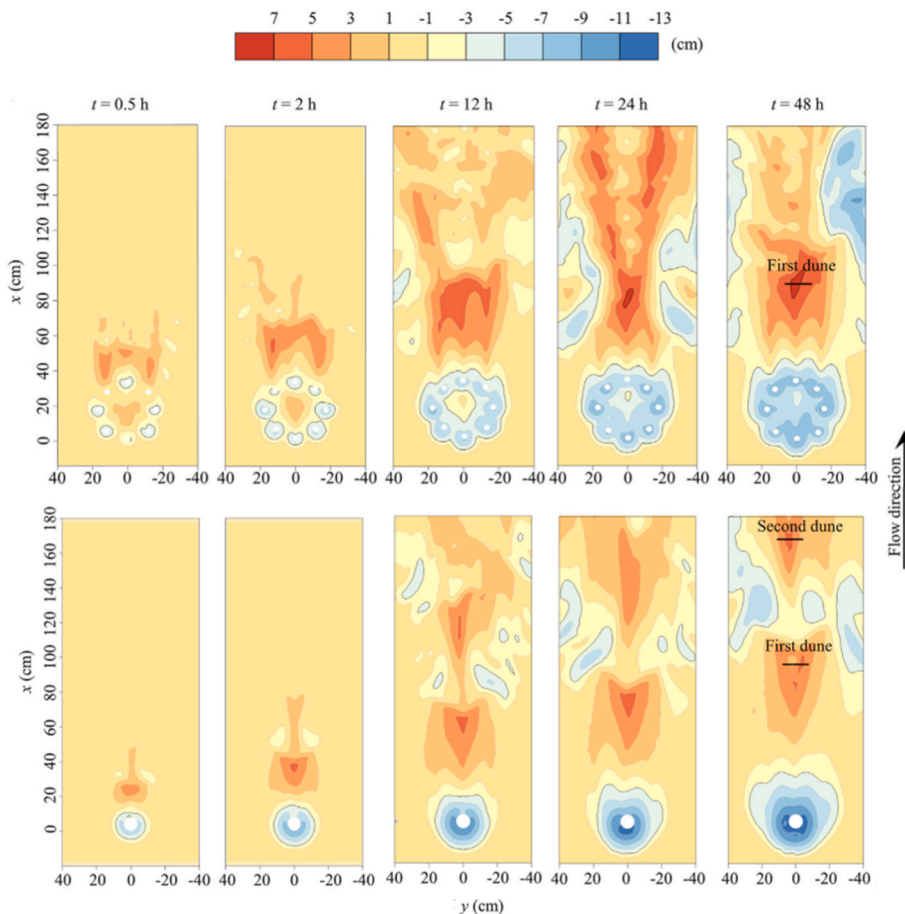

Fig. 19. Scour comparison between a High-Rise Structure Foundation (HRSF) and a Monopile – Reprinted with permission from Xiao et al. (2020), Copyright 2020, Elsevier.

lower blockage ratio generates less scour. Regarding the deposition zone of the sediments, the distance to the foundation changes with the variation of the flow direction.

Although these studies provided valuable information and a good starting point regarding the scour in HRSFs, the fact is they only covered a limited range of conditions (currents). This review shows that a true misrepresentation of in-situ offshore conditions was made, thus highlighting the importance of extending testing conditions for the expansion of the scour protection design to this complex foundation.

3.5. Suction bucket foundations

Suction bucket foundations are skirted structures inserted into the seabed to anchor OWT and offshore platforms of oil and gas, used mainly in the North Sea for clay soils, that do not require seabed preparation and can cover a large range of water depths, from 5 m up to 60 m (Houlsby et al., 2005; Wang et al., 2018).

As monopiles demand an expensive installation, due to the use of heavy pile-driving equipment, this type of foundation offers an economical, simpler, quicker, and non-weather-dependent alternative (Houlsby et al., 2005; Houlsby and Byrne, 2000; Byrne et al., 2002). As the self-weight of the foundation is not enough to thrust the caisson into the seabed, a 'suction' technique, that consists of pumping out the water trapped within the caissons, is used to create a pressure differential across the top of the bucket (Houlsby et al., 2005; Houlsby and Byrne, 2000; Byrne et al., 2002). For cohesive soils, this technique is sufficient to drive the foundation. For sandy soils, the applied suction leads to an upward flow, that reduces the effective shear stress within the caisson, causing a scenario similar to a 'piping failure'. Therefore, the soil-bearing capacity around the rim of the caisson is reduced, allowing it to penetrate the soil (Houlsby et al., 2005; Houlsby and Byrne, 2000; Byrne et al., 2002). Moreover, a suction bucket foundation can be adapted to a variety of bottom-fixed foundations (monopile, jacket, tripods), Fig. 20, and may be removed completely from the seabed, unlike piled foundations (Byrne et al., 2002). The decommissioning and removal procedure is the exact reverse process of the installation, *i.e.*, the application of an overpressure inside the bucket caisson (Houlsby and Byrne, 2000).
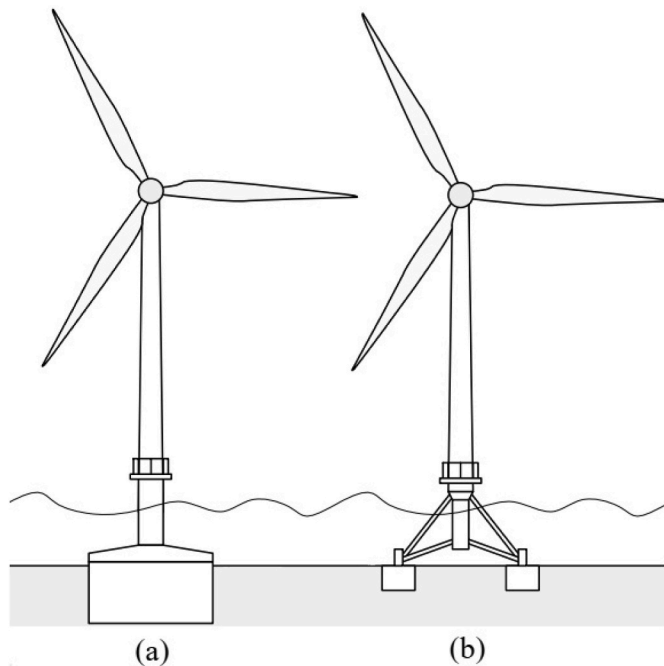
In the literature, most studies refer to the structural behaviour, the geotechnical design, or the effects of scour on the ultimate bearing capacity of the caisson that composes the foundation (Houlsby et al., 2005; Wang et al., 2018; Houlsby and Byrne, 2000; Byrne et al., 2002; Sturm, 2017; Guo et al., 2022; Ngo et al., 2023).

Houlsby et al. (2005) mentioned that since part of the suction bucket caisson could remain above the seabed, that could lead to more severe scour conditions. The results of small-scale physical model tests for a monopile bucket foundation, under irregular waves and tidal flows, were compared to the field analysis of decommissioned Horns Rev II and Dogger Bank suction bucket foundations (Stroescu and Frigaard, 2016; Stroescu, 2018). A good agreement between the field measurements (Table 4) and the experimental results (Table A5) was obtained, although the experimental campaign did not simulate the in-situ conditions from the considered sites. The results highlight that a suction bucket foundation could have in fact a lowering effect on scour, due to the blockage effect of the caisson features and due to the backfilling of scour holes registered during in-situ surveys. These observations open the door to the possibility of not including scour protections (Stroescu and Frigaard, 2016; Stroescu, 2018).

Another study regarding scour in a suction bucket foundation was performed by Yu et al. (2019) while testing a composite bucket foundation model under current-only, wave-only, and combined wave-current conditions. The following main conclusions were drawn.

- For the current-only tests, small sediment deposits were formed in front of the model, while scour was detected on both sides of the foundation and at the leeward side of the foundation (two scour "spoon-shaped" pits symmetrically distributed);
- Wave-only tests registered lower scour depths when compared to the currents-only and wave-current tests. As far as the seabed model topography, a strip-shaped deposition area perpendicular to the wave direction was detected 15 cm in front of the foundation. Two scour holes also appeared, one in front of the model, between the caisson and the strip-shaped dune, and the other at the downstream side of the model in the direction of the centre axis;
- For the wave-current tests, scour was detected in front and around the sides of the foundation, causing the exposure of the bucket skirt. A long and narrow scour hole also appeared behind the model, caused by the horseshoe vortex. When compared to the current-only test results, scour depths were lower, but the scour extent was higher;
- Relative scour depth and the horseshoe vortex influence increased with increasing KC values, consistent with scour development at monopile foundations.

As mentioned in Chapter 3.1, a novel foundation was introduced by Welzel et al. (2024), a 6-legged jacket gravity-based suction bucket foundation (Fig. 21). The foundation consists of a jacket with six legs each one with a large container, serving two purposes – offering buoyancy during transportation to the installation site and improving stability by adding weight inside the containers, after installation. To increase the stability even further, the complex foundation is inserted into the seabed using suction buckets. The research aim of Welzel et al. (2024) was to assess the influence of the complex geometric features of the new foundation and compare it to a standard 4-legged jacket. The large containers, due to the large containers, have a substantial blocking effect on the flow, leading to enhanced flow contractions and velocities. The laboratory tests were performed using only currents. For clear-water conditions (Fig. 21) local scour was more prominent than global scour. A

Fig. 20. - Suction bucket foundation for: a) Monopile, b) Tripod - adapted from Houlsby et al. (2005).

Table 5
Influence of rotor radius on scour for $C/H_r = 0.5$ Sun et al. (2018).

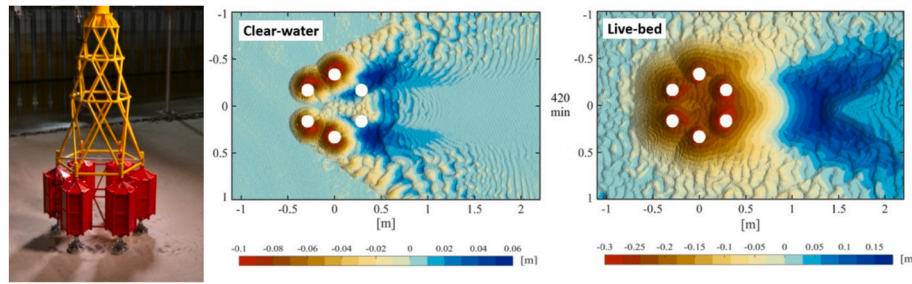| Rotor radius	37.4 mm	45.9 mm	56.3 mm
S/D_{pile}	2.6	2	2.2
Scour relative to a pile ($S/D_{pile} = 1.45$)	+78.9%	+37.5%	+51.3%

Fig. 21. Scour patterns for a 6-legged jacket gravity-based suction bucket foundation, under clear-water (left) and live-bed conditions (right): Scour – red and orange; Sediment depositions – adapted from Welzel et al. (2024).

maximum scour depth and extent of $0.81D_{caisson}$ and $3.46D_{caisson}$, respectively, was developed around the front and middle piles, while some sediment accumulation around the two downstream piles occurred. For live-bed conditions, the initial local scour holes merged into a singular scour hole and the deposition dune shifted to a distance around $9.8D_{caisson}$ towards downstream of the foundation, similar to the scour pattern around a pile group or even as in HRSFs (Fig. 19). The global scour hole has an extent of $10.8D_{caisson}$, the scour depth at the piles ranges between $2D_{caisson}$ (front and middle) and $2.3D_{caisson}$ (downstream piles), and the maximum scour depth at the centre of the structure is equal to $1.7D_{caisson}$. The results allowed to conclude that.

- For both structures, global scour develops mainly under live-bed conditions. For clear-water conditions, global scour was not intensively observed, an indicator that structural elements and features have little influence;
- Scour development to pile diameter progresses faster in the 4-legged jacket than at the 6-legged jacket gravity based suction bucket foundation;
- For clear-water conditions, the normalized sediment displacement and mean spatial distribution for both foundations were comparable, if the structures' reference diameter and footprint were also normalized;
- For live-bed conditions, spatial scour depth, relative to the 6-legged foundation's footprint, was 2.5 times higher when compared to the standard 4-legged jacket, showing that a significant increase in complexity and blockage ratio of the foundations leads to a non-proportional increase in sediment erosion;
- The local and global scour development at the 6-legged foundation, under live-bed conditions is very much aligned to the scour depths, extent, and shapes observed for an array of piles or even for HRSF;

4. Marine energy converters and hybrid foundations

Nowadays, OWTs and marine harvesting technologies have seen an increasing growth in attention by the private and scientific community in the marine renewable energy sector.
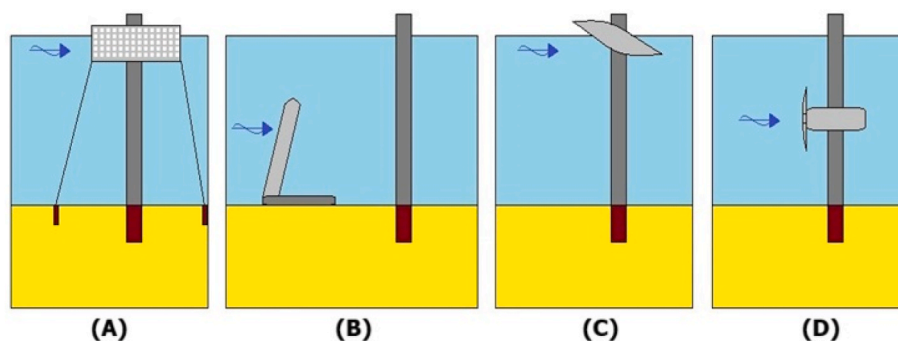
The energy crisis and climate changes are enhancing the demand, exploration, and investment in hybrid foundations that can combine more than one energy harvesting technology, for example, offshore wind turbines with marine energy converters being in the same foundation or floating platform (Fig. 22). These hybrid systems could optimize and boost power and energy production per structure. The question that arises is whether energy converters could shelter OWTs against waves, currents, and tides, or if they could increase loads, turbulence, and scour mechanisms (downflow, horseshoe, and/or lee-wake vortices) around the foundation.

Most of the new hybrid foundations combine floating OWTs with WECs or TECs. Since this article focuses on complex and hybrid bottom-fixed foundations, other studies are highly recommended for an extensive review of multiple floating hybrid solutions that have been adopted or are still in the development stage (Saeidtehrani et al., 2022; McTiernan and Sharman, 2020; Taveira-Pinto et al., 2021).

For bottom-fixed hybrid foundations, scour is a topic that has some knowledge gaps (Fazeres-Ferradosa et al., 2021) and, as it happens in OWT complex foundations, scour protection studies are still non-existent. The main focus has been the study of efficiency and hydrodynamic performance of converters and not so much on the scour behaviour in complex foundations. Nonetheless, scour protections in hybrid foundations remain an important topic of research, since.

- scour represents a threat to the offshore wind structure and the functioning of marine energy converters;
- the eventual accretion of sediments between the converter and the foundation could also lead to an efficiency decrease or malfunctioning of the device, thus reducing its viability;
- the implementation of marine energy converters could lead to softer scour countermeasures, hence reducing costs and expenditures;
- an effective scour protection could optimize the structural behaviour, thus enhancing the usage of hybrid foundations.

The literature points out a large knowledge gap regarding the usage

Fig. 22. - Conceptual schemes for possible hybrid OWT foundations, by combining: (A) aquaculture cage, (B) oscillating wave surge converter, (C) wave energy converter, and (D) tidal/current energy converter – not at scale.

and design of scour protections in hybrid foundations.

4.1. Marine energy converters

As aforementioned, the synergy between OWT and marine harvesting technologies presents new challenges and research topics. The movement of an oscillatory/rotative body, causes additional soil-fluid-structure interactions, since wave-orbital and current velocities change, as downflow pressures and vortices, in the vicinity of the structure. Standard scour patterns and behaviour in offshore foundations are no longer applicable. Therefore, scour protections – static or dynamic – designed under the actual knowledge, could be misadjusted.

The assessment of the actual design methods for marine energy converters or hybrid foundations should include other variables, and not just structural parameters (D_{50}, ρ_s, extent, thickness, S/D) and environmental parameters (d, H_s, T_p, U_c, U_m). They should consider cyclical variations of pressure caused by the device movement/oscillation and the influence that vibration increments could have on the natural frequency of the structure. The impact that the converter motion causes in soil properties, disturbance of current and tidal velocities, and variations in the flow field, are also other aspects that could produce some major influences in the design of hybrid foundations and scour protection mechanisms.

4.1.1. Wave energy converters (WECs)

An example of a wave energy converter that enforces a cyclical variation of movement and pressure, is the CECO converter (Rosa-Santos et al., 2019a). By converting its inclined motion into energy, a cycle of upward and downward pressure is started (Fig. 23), interfering with the flow field, enhancing and decreasing velocities, pressures, horseshoe, and lee-wake vortices near the profile bed, mainly behind the foundation (Fazeres-Ferradosa et al., 2021). Moreover, the movement itself could lead to excessive vibratory motion of the pile that supports the WEC. However, there is a possibility that by absorbing and reducing wave heights, the device could reduce scour at the foundation. The uncertainty of those facts would ask for reinforced scour protection or a softer countermeasure, which should be a motive for further exploratory research to assess if both structures – a CECO converter and an offshore foundation – could be advantageous to each other.

Another WEC that could have a positive impact as a scour corrective solution is the Oscillating Wave Surge Energy Converter (OWSEC) similar to a floating plate (Fig. 24), Zhu et al. (2020). This research assessed the implications and viability of such an energy converter as a
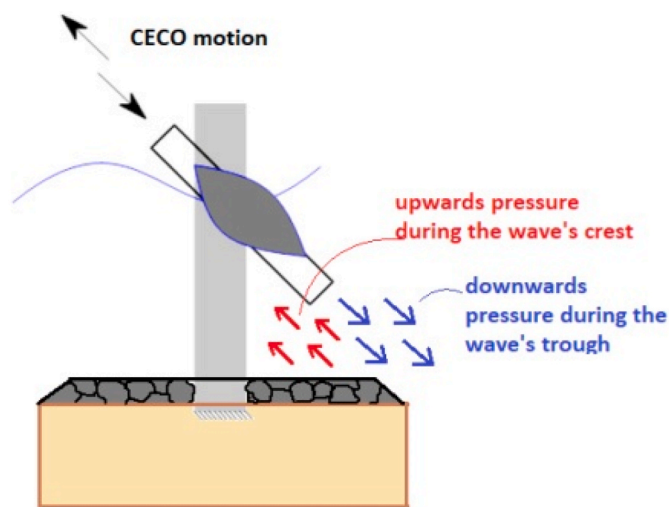
protective measure for a pipeline. It concluded that the device could work as a scour-reducing device, depending on characteristics such as size, motion, and other parameters. Thus, the influence of the flap rotation angle (α), wave height-water depth ratio and water depth-wavelength ratio on seabed changes were also studied (Taheri et al., 2022). By performing a set of tests, it was concluded that.

- by changing α, from motionless to a rotational body, scour was reduced in length and range, by moving scouring and deposition zones closer to the structure;
- by increasing α, the flap rotation reduces velocities leading to less scour and more deposition of sediments. But closer to the device, the flap motion and flow disturbances occur and vortices are created, so the scour behaviour is different;
- by increasing the H/d ratio, scour and bed level variations aggravate, concluding that shallow waters or more energetic wave conditions are detrimental to the scour defensive performance of the energy converter.

Therefore, it can be concluded that flap energy converters, when compared to similar fixed structures, decrease scour in the seabed, being a potential good scour countermeasure. However, scour protection might be required to protect the WEC from the problems that may arise from scour in its own foundation.

It should be also worth mentioning that a new floating two-flap OWSEC system (Fig. 25) has been tested by Ruehl et al. (2019), Coe et al. (2020), and Bosma et al. (2016), the so-called Floating Oscillating Surge Wave Energy Converter (FOSWEC). At an initial testing stage, the device was attached to a constraint platform that could lock/unlock different allowable degrees of freedom (DOF), Ruehl et al. (2019) and Bosma et al. (2016). In the second stage, the device was tested using mooring lines (Coe et al., 2020). Loads, the motion of the flaps, platform, and mooring behaviour, power-take-off (PTO) components, and incident wave fields were characterized using irregular/regular wave response tests. The implementation of a similar bottom-fixed version could be an interesting upgrade as a scour countermeasure to single-flap OWSEC.

Oscillating water columns (OWC) have been studied quite extensively in the last few years. Mainly integrated on breakwaters or sea walls, some literature research analysed scour patterns for gravity-based OWC-WEC (Lancaster et al., 2020, 2022). A detailed review of the findings can be seen in Fazeres-Ferradosa et al. (2021). However, the model was updated by adding two lateral pontoons, flop valves, and a chamber flap door (Lancaster et al., 2022). By testing different configurations of the pontoons, and the presence/absence of chamber doors, for different sets of conditions, it was concluded that.

- Even with the presence of the pontoons, scour compromised the back corners of the structure, for all the conditions tested, since downstream scour is regulated by flow contractions and vortex developments;

Fig. 23. – Scheme of CECO's movement and expected upward/downward pressure action on a scour protection – adapted from Fazeres-Ferradosa et al. (2021).
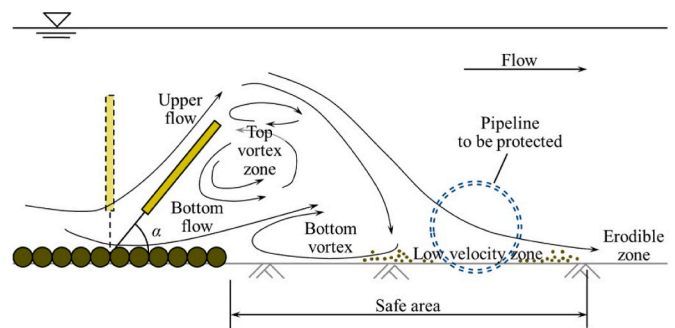
Fig. 24. – Scheme of the working mechanism of a bottom-mounted Oscillating Wave Surge Energy Converter (OWSEC), Zhu et al. (2020).
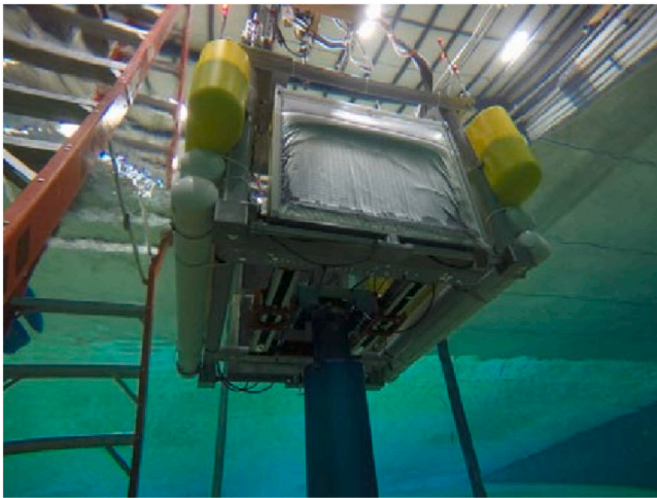
Fig. 25. - Underwater view of the Floating Oscillating Surge Wave Energy Converter (FOSWEC) – (Bosma et al., 2016).

- curve-edged pontoons represented a 23% scour reduction when compared to sharp-edged pontoons;
- the scour hole formation led to settlements of the structure.

These findings indicate that a hydrodynamic structural improvement of energy converters and offshore foundations could decrease scour in their vicinity, leading to the need for new, softer scour protective measures. Moreover, both studies advise some form of seabed preparation or scour protection to prevent settlements. These observations are aligned with the conclusions drawn in Van Velzen et al. (2016). Van Velzen and Bruinsma (2017), and Bruinsma et al. (2018).

4.1.2. Tidal current energy converters (TECs)

As WECs have shown to be a viable option to reduce scour when combined with OWT. TECs, on the other hand, represent a meaningful challenge since they induce some effects – the rotor may block the flow causing acceleration in current velocities, the wake effect of the turbine may alter hydrodynamics, and the enhanced turbulence could increase shear stress at the seabed vicinity –, thus enhancing scour around the structure (Chen and Lam, 2014; Kang et al., 2012; Neill et al., 2009). However, scour protection studies in TECs are non-existent to the authors' knowledge, but there is some information on scour in TECs, based mainly on the experience with ships' propellers or turbines fixed on single piles.

The rotor's effect, the increased wake effect under the turbine, and the tip clearance – the distance between the tip of a rotating blade to a stationary part, point, or object – are pointed out as the main considerations for scour induced by TECs (Chen and Lam, 2014). These facts are reinforced by Chen et al. (2017), which studied the influence of tip clearance on scour for a pile-supported horizontal axis turbine. The rotative movement of turbines has been proven to increase local velocities downflow, and the occurrence of horseshoe vortices, causing an amplification of shear stresses (Chen et al., 2017; Hill et al., 2014; Sun et al., 2018). By comparing three different tip clearance distances, results showed that lower distances to the bed profile lead to a faster scour extent of up to $1D_t$ downstream, and $0.5D_t$ from both sides (Chen et al., 2017).

A similar research on a Darrieus-type vertical axis turbine to assess scour parameters was developed for different tip clearance distances but also for distinct turbine radius (Sun et al., 2018). The results were in line with Chen et al. (2017), as the decrease in the tip clearance also led to higher scour rates – a 10%–20% increase in scour extent, and a 30% increase in scour depth. Moreover, it was concluded that equilibrium scour is independent of tip clearance, since a continuous decrease of the

distance to the sediment bed, at a certain point, does not translate to a significant increase in scour depth – the live bed scour effect takes control.

Considering the influence of the rotor radius, it was concluded that with the radius increment, maximum scour depths decrease at first and then increase (Sun et al., 2018) – Table 5; as for the tip clearance, scour increases in depth and extent with the decrease of the parameter (Table 6).

The maximum scour depth was achieved for a small rotor radius and when $C/H_r = 0.5$ – tip clearance distance (C), the height of the turbine rotor (H_r), Sun et al. (2018). As for the minimum scour ($1.6D$), it was obtained for the maximum rotor radius when the distance to the bed was equal to the height of the rotor. This is an indication that to minimize the prejudicial effect that TECs have on scour, the inclusion of these devices on OWT should be placed at a relatively high distance from the seabed.

The performance analysis of TECs by Chen et al. (2017) and Sun et al. (2018) was only carried out under currents. The results presented in Table 5 proved that tidal current devices can be detrimental to offshore foundations, reinforcing the idea and necessity of scour protections (Chen et al., 2013). The empirical formulas to predict scour in tidal current turbines (Chen et al., 2017; Sun et al., 2018), are a good starting point to build new proposals for scour protections for TECs.

A scour reduction using a tidal current turbine (TCT) was assessed by Charlier (2003) when implemented at an optimal position in front of a monopile facing the currents. In addition to reducing shear stress, the device also reduced the maximum depth of scour. It was indicated that scour evolves slower and is amplified further away from the rotor when the device is placed downstream of the foundation (Hill et al., 2014). This evidence was also detected by Yang et al. (2021) when using a numerical and physical model of a TCT on the sea-side of a monopile (1:12 scale factor). By varying the distance of the TCT to the foundation (10–50 cm) and the tip clearance distance to the seabed (5–25 cm), Fig. 26, for the same rotor speed and current velocity, it concluded that the device had the potential of reducing scour around the foundation (mainly in front and on both sides of the monopile). When properly installed, with an optimal distance of 30 cm to the turbine and 10 cm to the seabed, the TCT reduced the maximum shear stress on the seabed by 8% and the maximum scour depth by 42%. However, when placed closer or further away from this optimal position, scour depths and shear stresses reached similar rates to the control model (without the use of the converter). Hence, Yang et al. (2021) highlights that the scour mitigation effects of this type of device is highly conditioned to its installation position, to the tidal current speed, and to the rotor speed. Therefore, the author suggests that the implementation of such device in an OWT foundation should be done by carefully selecting its rotational speed and position taking into consideration different tidal current conditions.

These opposite opinions enhance the necessity to perform further research to clarify some contradictions and to ensure that scour protections can be accounted for in the optimization of tidal current energy converters.

4.2. Hybrid foundations

In literature, it is found the inclusion of WECs in maritime structures such as breakwaters, sea walls, and harbours, among others. It was concluded that for the toe region, erosion and sediment transport due to

Table 6
Influence of the tip clearance on scour for the same rotor radius ($H_r = 56.3$ mm), Sun et al. (2018).

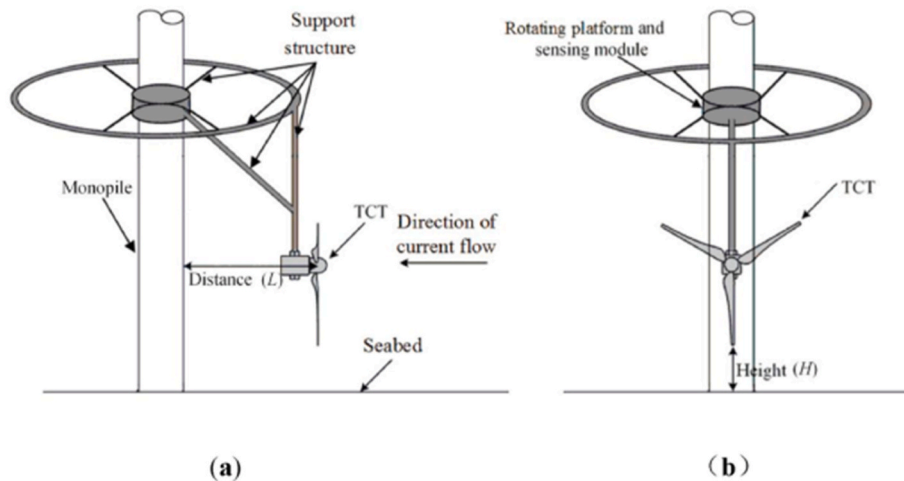| C/H_r	1.00	0.75	0.50	0.25
S/D_{pile}	1.6	1.7	2.2	2.2
Scour relative to a pile ($S/D_{pile} = 1.45$)	+9.9%	+16.8%	+51.3%	+51.3%
Scour extent (downstream)	4.6D	4.8D	8.5D	10.0D

Fig. 26. Three-bladed TCT device: (a) side view, (b) front view – Reprinted with permission from Yang et al. (2021), Copyright 2020, Elsevier.

wave reflection, breaking, and splashing is increased (Mustapa et al., 2017). Therefore, countermeasures against scour in these types of structures are necessary.

A model of a hybrid system by integrating a WEC into a rubble-mound breakwater to assess the stability under extreme onshore conditions was performed by Rosa-Santos et al. (2019b). Although no scour was detected at the end of 6000 waves, despite some block movements at the toe, Rosa-Santos et al. (2019b) looked for potential scour at the structure by including an energy converter.

Nevertheless, a soft scour countermeasure by adding a coastal cage net for aquaculture on an offshore jacket was implemented (Hsin-Hung et al., 2014). The concept of offshore aquaculture has been developed in the last few years and has gained a lot of momentum. The conclusions drawn help prevent scour around the foundation. For a 100-year return period wave-current condition, the maximum scour depth was reduced from 1.17D (without the cage) to 0.75D and 0.71D – one cage at the current side and one net at the current side and another at the wave side, respectively – representing a 35%–39% scour depth reduction (Hsin-Hung et al., 2014).

A combination of an OWSEC with an OWT foundation (monopile and GBF), under waves and currents for layered soils was used to assess scour by Miranda (2022). The study integrated the device at the upstream side of the foundations (Fig. 27). For a set of conditions (Table A6), the converter was placed at further distances from both foundations. The results obtained were compared to a setup without the device. A 16 set of tests for a geometrical scale of 1:50 resulted in Table A6.

Overall, several results reported an average reduction of the scour depth – 60% and 33% for the monopile and GBF, respectively – obtained with the presence of the wave flap energy converter in front of both foundations for a fine sand seabed (Miranda, 2022). As for layered soil, a decrease of 65% (monopile) and 67% (GBF) on the scour depth was registered. Even though scour protection was not incorporated, the values suggest that this approach could and should be considered as a scour countermeasure. It seems to be viable and could lead to the implementation of less extensive and thicker riprap protection, reinforcing that static protections may not be necessary, leading to considerable cost reductions.

Furthermore, Miranda (2022) states that:

- for the monopile, scour depth presented a higher value for fine sand instead of for the layered soil, without the device. With the presence of the WEC, that difference between scour depth for fine sand and layered soil was dissipated;
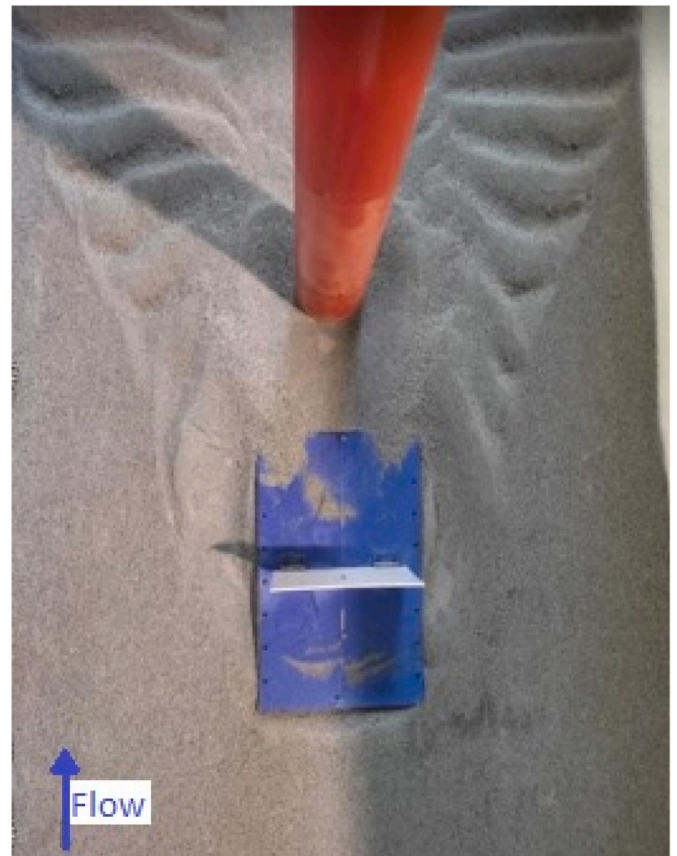
Fig. 27. Monopile and Oscillating Wave Surge Energy Converter (OWSEC) tested by Miranda (2022).

- for the GBF, without the OWSEC, the scour depth for both soils was similar. As a result of implementing the device, the layered soil experienced lower values of scour.

As a result of these findings, it is suggested that each case should be evaluated individually. To mitigate the differences in scour depth for each foundation in each soil combination, scour protections can play a significant role.

In summary, the literature shows a clear lack of research on scour protections for marine harvesting technologies and hybrid foundations.

Those subjects need to be properly addressed to optimize the design and implementation of these structures. The understanding of each specific interaction that those devices have between each other and with the seabed is fundamental. Depending on the offshore environmental conditions, certain energy converters may increase or decrease scour around such structures. The comprehension of scour phenomena when energy converters are applied could lead to novel concepts of scour protection, essential to the preservation of the structure. Since cost expenditures are still the decisive variable in the implementation of such alternatives, each energy converter needs to be addressed individually in the design initial stage. A future correct combination of energy converter-OWT foundation-scour protection can lead in fact to a significant cost reduction and improvement of the foundation's stability and competitiveness of offshore renewables.

5. Conclusions

This article aims to review the latest outcomes of the scour phenomena and protections related to the presence of offshore and marine harvesting technologies, to summarize the most recent knowledge gaps and research performed namely on offshore wind turbine foundations, with a special focus on complex and hybrid bottom-fixed foundations. Several challenges and potential future developments were identified, as a brief analysis of the most recent developments on scour protections for OWT. It was intended to show that the different topics here listed can support and serve as a basis for upcoming research, development, and optimization of scour protections for complex and hybrid OWT foundations in a marine environment, possibly leading to lower costs and higher performances of offshore and marine harvesting technologies.

From this review, the following conclusions can be presented.

- The study of scour around monopiles has been extensively covered in the literature. In recent years, the discussion regarding scour on complex bottom-fixed foundations has grown, still, some of the approaches used in actual situations are monopile-related. There is a need for further understanding, as higher global and local scour depths were detected in complex structures when compared to the average monopile scour depth (Welzel, 2021);
- There is a lack of a general understanding of the scour development at complex structures. Most studies only analyse the evolution of equilibrium/maximum scour depths, thus neglecting a deeper analysis of the time scale, spatial scour depth variations, erosion/deposition patterns, the interaction between local and global scour, and the influence of the complex structural design features on the spatial scour depth changes;
- The prediction of scour effects frequently relies on simplified hydraulic conditions, waves and/or currents. There is a lack of knowledge on the effects of real hydraulic conditions, such as the simulation of tidal flow conditions or the influence of multidirectional waves, on the scouring process;
- Traditionally, static scour protections are the most utilized and studied type of protection, despite being based on some sort of empirical concepts. Less expensive optimizations, such as dynamic or wide-graded alternatives, are not fully developed or studied, at the same level of knowledge, nor have been extensively addressed for complex foundations, marine energy converters, and hybrid foundations;
- Design formulas heavily based on monopiles are still used or adapted, even though scour behaviour, flow field modifications, blockage effects, and loads around complex structures are different;
- The scour protection stability assessment is a crucial part of the design procedure. Nonetheless, only a few studies have focused on major improvements regarding the stability evaluation, damage characterization, and the scale effects associated with the application of small-scale physical model tests;

- Absence of access to data, result discussions, reports, and information in situ, that are retained by stakeholders, due to confidential policies, harms the development or optimization of (new) scour protection design formulas;
- Although the number of studies that have used numerical models has been increasing in recent years, scour protection numerical models are still a huge field of study yet to be covered. The majority of the models focus on the structural behaviour of bottom-fixed or floating foundations;
- Most studies regarding marine harvesting technologies focus on hydrodynamics and performance improvement over scour and protections. No studies are reporting the use of scour protections, and scour research considers only waves for WECs or tidal currents for TECs, a miss-representation of real marine environmental conditions;
- Scour studies in hybrid structures are scarce and almost non-existent, even with the high potential that the application of energy converters in offshore wind turbines can offer. A synergy between both could contribute to a cost reduction, to the creation of new energy sources that in the end could increase the competitiveness of the renewable energy sector and devote to the reduction of the electricity price;
- Knowledge gaps and lack of reports in the literature on the combination of WECs or TECs with OWTs can lead to the increase or reduction of scour effects in the foundation.

As a final note, there is a clear absence of works that performed physical and numerical modelling of scour protections for complex and hybrid bottom-fixed foundations, and marine harvesting technologies. Although some encouragements have been made regarding the understanding of scour development and prediction formulas on OWT complex foundations and marine energy converters, the authors recognize that the future of scour research in the offshore sector involves the necessity of identifying new and specific design formulas and countermeasures for (dynamic) scour protections for these types of foundations and structures.

CRediT authorship contribution statement

J. Chambel: Writing – review & editing, Writing – original draft, Methodology, Formal analysis, Conceptualization. **T. Fazeres-Ferradosa:** Methodology, Conceptualization, Project administration, Writing – original draft, Writing – review & editing. **F. Miranda:** Writing – review & editing. **A.M. Bento:** Writing – review & editing. **F. Taveira-Pinto:** Project administration, Writing – review & editing. **P. Lomonaco:** Writing – review & editing.

Declaration of competing interest

The authors declare that they have no known competing financial interests or personal relationships that could have appeared to influence the work reported in this paper.

Data availability

No data was used for the research described in the article.

Abbreviations

A	Reference distance times the structure footprint length
A_{front}	Reference distance relative to the structure's upstream side
A_{rear}	Reference distance relative to the structure's downstream side
A'	Equation (8) additional term
a_0, a_2, a_3	Regression fitting coefficients
a_1, a_4	Coefficient for hydrodynamic conditions
B	Jacket lowest node distance impact coefficient
B'	Equation (7) additional term
B''	Equation (8) additional term
b_0	Regression fitting coefficient
C	Tip clearance distance
C'	Equation (7) additional term
c_1, c_2, c_3	Equation (11) regression fitting coefficients
D	Diameter
D*	Dimensionless grain size
$D_{caisson}$	Suction bucket caisson diameter
D_{cr}	Critical stone size
D_{base}	Diameter of a non-uniform cylindrical structure
D_e	Equivalent diameter
D_{n50}	Nominal stone diameter of the scour protection
D_p	Pile diameter
D_t	Turbine disc diameter
D_{15}	15th percentile of scour protection material grading
D_{50}	Mean stone diameter of the scour protection material
$D_{67.5}$	67.5th percentile of scour protection material grading
D_{85}	85th percentile of scour protection material grading
d	Water depth
d_p	Diameter HRSF individual piles
d_s	Local scour depth for HRSF piles
d_{se}	Equilibrium scour depth for HRSF individual piles
Eu	Euler number
Fr	Froude number
G	Pile gap
g	Gravitational acceleration
H	Wave height
H_m	Mean wave height
H_{m0}	Spectral significative wave height
H_r	Height of turbine rotor
H_s	Significant wave height
h	flow depth
KC	Keulegan-Carpenter number
k	wave number
kw	GSC volume factor
k_1	Velocity correlation factor
k'	HRSF location constant
l	GSC long edge length
N	Number of waves
Ns	Stability number
N_s*	Modified stability number
n	Number of HRSF piles
R	Protective strength ratio
Re_D	Structure Reynolds number
R'	Radial distance of the scour hole
S	Scour depth
S/D	Relative scour depth
S/D_{column}	Maximum relative scour depth under the column
S/D_{pile}	Maximum relative scour depth in the piles
S_{3D}	Damage number
$S_{currents}$	Equilibrium Scour depth under current-only

S_{eq}	Equilibrium scour depth
S_{end}/D	Relative maximum scour depth
S_{max}/D	Relative maximum scour depth at GBS's pontoons
s	specific density (ρ_s/ρ_w)
T	Wave period
T*	Dimensionless time scale
T_c	Time scale period
T_e	Equilibrium time scale for HRSF
T_m	Mean wave period
$T_{m-1,0}$	Energy wave period
T_p	Wave peak period
t	time step in scour process for HRSF
U_c	Depth averaged current velocity
U_{cr}	Mean threshold velocity of sediments
U_{cw}	Velocity ratio
U_m	Orbital bottom velocity
U_{max}	Vortice local maximum velocity
V	GSC volume
$V_{A,i}$	Cumulative erosion volume
$V_{A,max}$	Maximum erosion volume
V_{Area}	Areal development of volumes
V_c	Threshold sediment motion velocity
V_s	Scour Volume for HRSF
V_{se}	Equilibrium scour volume for HRSF
W	GSC weight
w_s	Settling velocity
α	Flap rotation angle
α_f	Amplification factor
α_{wc-mp}	Interaction angle between wave-current load and ACM-pipeline system
ζ	Function of hydrodynamic conditions
θ_{cr}	Critical Shields parameter
ρ	Density of the GSC
ρ_s	Density of rock material
ρ_w	Water mass density
τ_{cr}	Critical bed shear stress
τ_m	Mean combined bed shear stress (current and wave-induced)
τ_{max}	Maximum combined bed shear stress (current and wave-induced)
γ	GSC specific weight
Δ	Buoyant GSC density

Appendix A. Complex and Hybrid Foundations Physical Model Studies (Tables)

Table A.1
Physical modelling studies for jackets' scour protections – prototype values.

Reference	Sarmiento et al. (2021)	Bruinsma et al. (2018)	Hsin-Hung et al. (2014)
Scale	1:30	Full Scale	1:36
d (m)	39.93	[30.00, 32.30]	[12.00, 16.00]
T_p (s)	Not provided	[0.00, 12.50]	[7.00–11.74]
U_c (m/s)	50-year Return Period (exact value not provided)	[0.00, 1.20]	[0.00, 1.00]
Types of Waves	Irregular	Irregular	Irregular
H_s (m)	[1–50] year Return Period (exact value not provided)	[0.00, 8.90]	[2.50–7.72]
Duration	3 h (18 h cumulative)	Not provided	8 h
Wave-Current Direction	0°	Not provided	90°
D (m)	Not provided	Not provided	4-pile jacket (2.08 m diameter/pile)
Protection type	Riprap	Riprap	Riprap + Precast concrete blocks
D_{n50} (mm)	Not provided	[76.2–228.6]	Not provided
ρ_s (kg/m^3)	Not provided	3050	Not provided
Armour Thickness	Variable (but up to $5D_{50}$)	1 m	3 m (2 m embedded in the seabed)
Armour Extent	Not provided	12 m radius from each pile (square protection)	14 m radius from each pile (square protection)
Filter	–	–	Geotextile & Granular

Table A.2
Physical models and in-situ scour analysis for tripods – prototype values.

Reference	Stahlmann and Schlurmann (2010)		
Scale	1:40	1:12	1:1
d (m)	[24, 30]	30	28
T_p (s)	[9.5–19.0]	[9.6–19.1]	**In-situ measurements Conditions (50-year period): Waves:** $H_{s,50} = 8.5$ m, $H_{max,50} = 15.8$ m,
Types of Waves	Regular + Irregular	Regular + Irregular	$T_{p,50} = 12.3$ s
H_s (m)	[4–12]	[6.12–9.24]	**Currents:** $U_{c,50} = 1.3$ m/s, $U_{c,ground50} = 0.8$ m/s
Duration	[3000 to 6000] waves	[2500, 3000, 4000] waves	
D (m)	Not provided	Not provided	Not provided
S/D (Rear pile 1)	0.66	1.05	[1.1–1.4]
S/D (Rear pile 2)	0.67	1.03	
S/D (Front pile)	0.55	0.80	
S/D (under Main Columns)	–	1.11	2.5
S/D (Downstream)	0.92	0.31	–

Table A.3
Physical modelling studies for GBFs' scour protections – prototype values.

Reference	Wilms et al. (2012)	De Sonneville et al. (2014)	Chen et al. (2011)	Tavouktsoglou (2018)	Gao et al. (2023)
Scale	1:17	1:60	1:50	1:100	1:100
d (m)	37.5	[28.2, 29.3]	29	40	30
T_p (s)	13.8	[0.0–13.6]	Bora: 9.9 Scirocco: 12.0	[10.0–30.0]	[8.0–12.0]
U_c (m/s)	–	[0.30–2.00]	Normal direction: Bora: 0.53 Scirocco: 0.10 Inline direction: Bora: 0.07 Scirocco: 0.18	[-2.9 – 6.5]	[1.5–2.5]
Types of Waves	Irregular	Irregular	Irregular	Regular	Regular
H_s (m)	10.8	[0.0–10.0]	Bora: 5.3 Scirocco: 5.9	[0.0–16.0]	[5.5–8.5]
Duration	5000 waves	2000 waves 15.5 h (only currents)	18 h	10 000 waves 5 h (only currents)	3 h
Wave-Current Direction	–	0° Bidirectional	Bora: 60° Scirocco: 150°	[0°, 90°]	Waves or Currents: [0°, 90°]
D (m)	32.5	90 × 70 (rectangular)	Main Structure: 88 × 180 (rectangular) Mooring Dolphins: 56.4 × 28.4 (rectangular)	20	Main Structure: 70 × 90 (rectangular)
Protection type	Geotextile sand containers	Riprap	Riprap	Riprap	6 different systems
D_{n50} (mm)	Container: 2.05 m × 2.05 m	[250, 360, 420]	Not provided	[294, 546, 882]	760
ρ_s (kg/m^3)	Not provided	[2650, 3200]	Not provided	[2500, 2550, 2620]	1700
Armour Thickness	2 layers	5D_{n50} (initial) Varying (final)	Varying	Not provided	2.5D_{50}
Armour Extent	52.5 m (diameter)	118 m × 98 m (initial) Varying (final)	Varying	5D	1.25 to 1.5D
Filter	Not used	Granular (D$_{50}$ = 0.05 m)	Not used	Geotextile	Varying

Table A.4
Physical modelling studies for scour in HRSFs – prototype values.

Reference	Xiao et al. (2020)	Xiao et al. (2021)	Liang et al. (2021)
Scale	1:50	1:50	1:50
d (m)	7.5	[7.5, 12.5]	[5–12.5]
U_c (m/s)	1.96	[1.63–1.98]	[1.91–2.05]
Duration (model)	48 h	100 h	96 h
Current/Alignment angle	[0–22.55] °	[0–22.55] °	0°
D_p and D_e (m)	Monopile: 4 m 8-pile HRSF: 4.95 m 10-pile HRSF: 4.75 m	Monopile: 4 m 8-pile HRSF: 4.95 m 10-pile HRSF: 4.75 m	10-pile HRSF: 4.75 m
Bottom outer diameter (m)	Monopile: 4 m HRSF: 17 m	Monopile: 4 m HRSF: 17 m	HRSF: 17 m
S/D or S/D_e	Monopile: 1.56 8-pile HRSF: [0.96–0.98] 10-pile HRSF: [0.99–1.01]	Monopile: [0.45–1.71] 8-pile HRSF: [0.52–1.14] 10-pile HRSF: [0.48–1.10]	≈1.05

Table A.5
Physical modelling studies for Suction Bucket foundations – prototype values.

Reference	Yu et al. (2019)	Stroescu and Frigaard (2016), Stroescu (2018)	Welzel et al. (2024)
Scale	1:40 1:60	1:90	1:45
d (m)	[8, 10]	28.8	30.2
T_p (s)	[6.64–7.98]	[11.48–12.24]	–
U_c (m/s)	[1.11–1.27]	[1.71–3.98]	[1.61, 2.817]
Type of waves	Irregular	Irregular	–
H_s *(m)*	[1.2–2.4]	[4.5–9.0]	–
Duration (model)	Currents-only: 24 h Waves-only: 21 h Waves-Currents: 32 h	2 h	Currents-only: 7 h
Wave-Current direction	0°	[0, 90] °	currents-only: 0° (unidirectional)
$D_{caisson}$ (m)	30	18	5.85
$S/D_{caisson}$	Currents-only: [0.069, 0.134] Waves-only: 0.055 Waves-Currents: [0.066–0.144]	[0.05–0.4]	Clear-water regime: 0.81 Live-bed regime: [2–2.3]

Table A.6
Physical modelling study for a hybrid monopile & GBF foundation (Miranda, 2022) – prototype values.

Type of soil	Fine sand bed	Layered soil
Scale	1:50	
d (m)	18	
T_p (s)	[9.31–10.27]	[9.31–10.35]
U_c (m/s)	1.22	
Type of Waves	Irregular	
H_{m0} (m)	[4.65–5.1]	[4.4–4.85]
U_m (m/s)	[0.785–0.919]	[0.757–0.898]
U_{cw}	[0.570–0.608]	[0.575–0.616]
Duration	3000 waves	
Wave-current direction	0°	
D (m)	Monopile: 5.5 GBF: 9	
Converter	OWSEC: 7.5 m × 5 m flap	
Converter distance to the foundation	[7.5, 12.5, 17.5] m	
$S_{monopile}$	No WEC: 1.65 m WEC: [0.65–0.75] m	No WEC: 2.5 m WEC: [0.65–0.9] m
$S/D_{monopile}$	No WEC: 0.30 WEC: [0.12–0.14]	No WEC: 0.45 WEC: [0.12–0.16]
S_{GBF}	No WEC: 0.8 m WEC: [0.5–0.55] m	No WEC: 0.9 m WEC: [0.15–0.45] m
S/D_{GBF}	No WEC: 0.09 WEC: 0.06	No WEC: 0.10 WEC: [0.02–0.04]
Scour protection	Not applied	

References

Agrawal, A.K., Khan, M.A., Yi, Z., Aboobaker, N., 2007. Handbook of Scour Countermeasures Designs, 2007, New Jersey Department of Transportation.

Ahmad, N., Kamath, A., Bihs, H., 2020. 3D numerical modelling of scour around a jacket structure with dynamic free surface capturing. Ocean Eng. 200, 107104.

Aleksandrova, N., Emmanouil, A., Van Duren, L., 2023. Scale model testing of eco-friendly scour protections for offshore foundations and cables, 2023. In: Proceedings of the 11th International Conference on Scour and Erosion (ICSE-11). International Society for Soil Mechanics and Geotechnical Engineering (ISSMGE): Copenhagen (Denmark).

Amaechi, C.V., Reda, A., Butler, H.O., Ja'e, I.A., An, C., 2022. Review on fixed and floating offshore structures. Part I: types of platforms with some applications. J. Mar. Sci. Eng. 10 (8), 1074.

Baelus, L., Bolle, A., Szengel, V., 2018. Long term scour monitoring around offshore jacket foundations on a sandy seabed. In: *In Proceedings Of the Ninth International Conference On Scour And Erosion*. 2018. Taipei, Taiwan.

Beg, M., 2008. Effect of mutual interference of bridge piers on local scour. In: *Department Of Civil Engineering*. 2008. Aligarh Muslim University: Aligarh, India.

Bhattacharya, S., 2014. Challenges in design of foundations for offshore wind turbines. Eng. Techno. Ref. 1–9.

Bolle, A., de Winter, J., Goossens, W., Haerens, P., Dewaele, G., 2012. Scour monitoring around offshore jackets and gravity based foundations. In: *In Proceedings Of the Sixth International Conference On Scour And Erosion*. 2012. Paris, France.

Bosma, B., Ruehl, K., Simmons, A., Gunawan, B., Lomonaco, P., 2016. WEC-sim Phase 1 Validation Testing: Experimental Setup and Initial Results.

Breusers, H.N.C., 1972. Local Scour Near Offshore Structures. Publication, Delft Hydraulics Laboratory. Delft.

Bruinsma, N., Van Velzen, G., Riezebos, H., Tilmans, W.M.K., 2018. Scour Development and Conceptual Scour Protection Layout at OHVS HKN and HKWa, 2018, Deltares.

Byrne, B., Houlsby, G., Martin, C., Fish, P., 2002. Suction caisson foundations for offshore wind turbines. Wind Eng. 26, 145–155.

Chambel, J., 2019. Analysis of Long-Term Damage of Offshore Wind Turbine Foundations. University of Porto: Porto, Portugal, 2019.

Charlier, R.H., 2003. A "sleeper" awakes: tidal current power. Renew. Sustain. Energy Rev. 7 (6), 515–529.

Chen, L., Lam, W.-H., 2014. Methods for predicting seabed scour around marine current turbine. Renew. Sustain. Energy Rev. 29, 683–692.

Chen, Z., Hurdle, D., Kram, N., Lomonaco, P., Cornett, A., 2011. Design and Testing of Scour Protection for Adriatic LNG GBS.

Chen, L., Lam, W., Shamsuddin, A., 2013. Potential scour for marine current turbines based on experience of offshore wind turbine. In: IOP Conference Series: Earth and Environmental Science, vol. 2013. IOP Publishing.

Chen, L., Hashim, R., Othman, F., Motamedi, S., 2017. Experimental study on scour profile of pile-supported horizontal axis tidal current turbine. Renew. Energy 114, 744–754.

Chen, H., Zhang, J., Wang, F., Guo, Y., Guan, D., Feng, L., 2023. Experimental investigation of the current induced local scour around a jacket foundation. Ocean Eng. 285, 115369.

Coe, R., Bacelli, G., Forbush, D., Spencer, S., Dullea, K., Bosma, B., Lomonaco, P., 2020. FOSWEC Dynamics and Controls Test Report.

Coghlan, I., Collins, S., McLaren, R., Blacka, M., 2023. Stability Assessment Considerations for Articulated Concrete Block Scour Mats under Wave Attack.

Corvaro, S., Marini, F., Mancinelli, A., Lorenzoni, C., 2018. Scour Protection around a single slender pile exposed to waves. Coastal Eng. Proc 1 (36) papers.6.

De Sonneville, B., Van Velzen, G., Wigaard, J., 2014. Design and optimization of scour protection for offshore wind platform Dolwin Beta. In: *International Conference On Offshore Mechanics And Arctic Engineering*. 2014. American Society of Mechanical Engineers.

De Vos, L., 2008. Optimisation of scour protection design for monopiles and quantification of waver run-up. In: *Faculty Of Engineering*. 2008. Ghent University, Belgium, p. 278. Ghent.

De Vos, L., De Rouck, J., Troch, P., Frigaard, P., 2011. Empirical design of scour protections around monopile foundations: Part 1: static approach. Coast Eng. 58 (6), 540–553.

De Vos, L., De Rouck, J., Troch, P., Frigaard, P., 2012. Empirical design of scour protections around monopile foundations. Part 2: dynamic approach. Coast Eng. 60, 286–298.

den Boon, J.H., Sutherland, J., Whitehouse, R.J.S., Soulsby, R.L., Stam, C.J.M., Verhoeven, K., Høgedal, M., Hald, T., 2004. Scour behaviour and scour protection for monopile foundations of offshore wind turbines. Proceed. European Wind Energy Conference & Exhibition. 14.

Fazeres-Ferradosa, T., Taveira-Pinto, F., Rosa-Santos, P., Chambel, J., 2019a. A review of reliability analysis of offshore scour protections. Proc. Institution of Civil Eng. - Maritime Eng 172 (3), 104–117.

Fazeres-Ferradosa, T., Taveira-Pinto, F., Rosa-Santos, P., Chambel, J., 2019b. Probabilistic comparison of static and dynamic failure criteria of scour protections. J. Mar. Sci. Eng. 7 (11), 400.

Fazeres-Ferradosa, T., Chambel, J., Taveira-Pinto, F., Rosa-Santos, P., Taveira-Pinto, F.V. C., Giannini, G., Haerens, P., 2021. Scour protections for offshore foundations of marine energy harvesting technologies: a review. J. Mar. Sci. Eng. 9 (3), 297.

Fredsoe, J., Deigaard, R., 1992. Mechanics of Coastal Sediment Transport, vol. 3. World scientific publishing company.

Gao, Y., Chen, W., Zhou, P., Du, F., Wang, L., 2023. Experimental investigation on scour development and scour protection for offshore converter platform. Mar. Struct. 90, 103440.

Grüne, J., Sparboom, U., Schmidt-Koppenhagen, R., Oumeraci, H., Mitzlaff, H.A., Uecker, J., Peters, K., 2006a. Innovative scour protection with geotextile sand containers for offshore monopile foundations of wind energy turbines. In: *3rd International Conference On Scour And Erosion (ICSE)*. 2006.

Grüne, J., Sparboom, U., Schmidt-Koppenhagen, R., Wang, Z., Oumeraci, H., 2006b. Large-scale investigations of geotextile sandcontainers used for scour protection of offshore monopiles supporting wind energy turbines. In: 25th International Conference on Offshore Mechanics and Arctic Engineering, vol. 2006. OMAE).

Grüne, J., Sparboom, U., Schmidt-Koppenhagen, R., Wang, Z., Oumeraci, H., 2006c. Stability tests of geotextile sand containers for monopile scour protections. In: 30th International Conference on Coastal Engineering (ICCE), 2006.

Guo, X., Liu, J., Yi, P., Feng, X., Han, C., 2022. Effects of local scour on failure envelopes of offshore monopiles and caissons. Appl. Ocean Res. 118, 103007.

Haritos, N., 2007. Introduction to the analysis and design of offshore structures–an overview. Electron. J. Struct. Eng. (1), 55–65.

Harris, J., Whitehouse, R., 2014. Marine scour: lessons from nature's laboratory. Scour 766, 19.

Heibaum, M., Trentmann, J., 2010. Partial grouted riprap for enhanced scour resistance. In: Burns, S.E., Bhatia, S.K., Avila, C.M.C., Hunt, B.E. (Eds.), Proceedings 5th International Conference on Scour and Erosion (ICSE-5), November 7-10, 2010, San Francisco, USA. American Society of Civil Engineers, Reston, VA, pp. 1–10, 2010.

Hill, C., Musa, M., Chamorro, L.P., Ellis, C., Guala, M., 2014. Local scour around a model hydrokinetic turbine in an erodible channel. J. Hydraul. Eng. 140 (8), 04014037.

Houlsby, G., Byrne, B., 2000. Suction caisson foundations for offshore wind turbines and anemometer masts. Wind Eng. 24, 249–255.

Houlsby, G., Ibsen, L., Byrne, B., 2005. Suction caissons for wind turbines. Int Symp Front Offshore Geotech 75.

Hoyme, H., Su, J., Kono, J., Wallbaum, H., 2018. *Nonwoven Geotextile Scour Protection at Offshore Wind Parks, Application and Life Cycle Assessment*: Scour and Erosion IX - Proceedings of the 9th International Conference on Scour and Erosion, ICSE, pp. 315–321.

Hsin-Hung, C., Ray-Yeng, Y., Hwung-Hweng, H., 2014. Study of hard and soft countermeasures for scour protection of the jacket-type offshore wind turbine foundation. J. Mar. Sci. Eng. 2 (3), 551–567.

Hu, R., Wang, X., Liu, H., Lu, Y., 2021. Experimental study of local scour around tripod foundation in combined collinear waves-current conditions. J. Mar. Sci. Eng. 9 (12), 1373.

Hu, R., Lu, Y., Leng, H., Liu, H., Shi, W., 2022a. A novel countermeasure for preventing scour around monopile foundations using Ionic Soil Stabilizer solidified slurry. Appl. Ocean Res. 121, 103121.

Hu, R., Wang, X., Liu, H., Leng, H., 2022b. Scour protection of submarine pipelines using ionic soil stabilizer solidified soil. J. Mar. Sci. Eng. 10 https://doi.org/10.3390/jmse10010076.

Hu, R., Wang, X., Liu, H., Chen, D., 2022c. Numerical study of local scour around tripod foundation in random waves. J. Mar. Sci. Eng. 10 (4), 475.

Hudson, R.Y., 1959. Laboratory investigation of rubble-mound breakwaters. J. Waterw. Harb. Div. 85 (3), 93–121.

Kang, S., Borazjani, I., Colby, J.A., Sotiropoulos, F., 2012. Numerical simulation of 3D flow past a real-life marine hydrokinetic turbine. Adv. Water Resour. 39, 33–43.

Kim, D., Jung, S., Na, W.-B., 2021. Evaluation of turbulence models for estimating the wake region of artificial reefs using particle image velocimetry and computational fluid dynamics. Ocean Eng. 223, 108673.

Kim, T., Kwon, Y., Lee, J., Lee, E., Kwon, S., 2022. Wave attenuation prediction of artificial coral reef using machine-learning integrated with hydraulic experiment. Ocean Eng. 248, 110324.

Lancaster, O., Cossu, R., Baldock, T.E., 2020. Experimental investigation into 3D scour processes around a gravity based oscillating water column wave energy converter. Coast Eng. 161, 103754.

Lancaster, O., Cossu, R., Wuppukondur, A., Moar, A.A., Hunter, S., Baldock, T.E., 2022. Experimental measurements of wave-induced scour around a scaled gravity-based oscillating water column wave energy converter. Appl. Ocean Res. 126, 103268.

Li, C., Chi, Y., Sun, X., Han, Y., Chen, X., Zhao, L., Zhang, H., 2017. Construction technology of high-rise pile cap foundation of offshore wind power in Taiwan Strait. IOP Conf. Ser. Earth Environ. Sci. 93, 012037.

Li, Y., Xu, Q., Li, Y., Li, Y., Liu, C., 2022a. Application of microbial-induced calcium carbonate precipitation in wave erosion protection of the sandy slope: an experimental study. Sustainability 14. https://doi.org/10.3390/su142012965.

Li, Y., Guo, Z., Wang, L., Yang, H., Li, Y., Zhu, J., 2022b. An innovative eco-friendly method for scour protection around monopile foundation. Appl. Ocean Res. 123, 103177.

Li, J., Guo, Y., Lian, J., Wang, H., 2023. Mechanisms, assessments, countermeasures, and prospects for offshore wind turbine foundation scour research. Ocean Eng. 281, 114893.

Lian, J., Li, J., Guo, Y., Wang, H., Yang, X., 2022. Numerical study on local scour characteristics of multi-bucket jacket foundation considering exposed height. Appl. Ocean Res. 121, 103092.

Liang, Z., Jeng, D.-S., Liu, J., Zhang, J., 2022. Numerical study of Articulated Concrete Mattresses (ACMs) for offshore pipeline protection. Ocean Eng. 255, 111467.

Liang, D., Jia, H., Xiao, Y., Yuan, S., 2021. Experimental investigation of turbulent flows around high-rise structure foundations and implications on scour. Water Sci. Eng. 15, 47–56.

López, I., Tinoco, H., Aragonés, L., García-Barba, J., 2016. The multifunctional artificial reef and its role in the defence of the Mediterranean coast. Sci. Total Environ. 550, 910–923.

Ma, H., Chen, C., 2021. Scour protection assessment of monopile foundation design for offshore wind turbines. Ocean Eng. 231, 109083.

Marin-Diaz, B., Fivash, G.S., Nauta, J., Temmink, R.J.M., Hijner, N., Reijers, V.C., Cruijsen, P.P.M.J.M., Didderen, K., Heusinkveld, J.H.T., Penning, E., Maldonado-Garcia, G., van Belzen, J., de Smit, J.C., Christianen, M.J.A., van der Heide, T., van der Wal, D., Olff, H., Bouma, T.J., Govers, L.L., 2021. On the use of large-scale biodegradable artificial reefs for intertidal foreshore stabilization. Ecol. Eng. 170, 106354.

Matutano, C., Negro, V., Lopez-Gutierrez, J.S., Esteban, M.D., 2013. Scour prediction and scour protections in offshore wind farms. Renew. Energy 57, 358–365.

McTiernan, K.L., Sharman, K.T., 2020. Review of hybrid offshore wind and wave energy systems. In: *Journal Of Physics: Conference Series*. 2020. IOP Publishing.

Miranda, F., 2022. *Experimental Study On Scour Around Foundations For Marine Harvesting Technologies In Complex Soils*. 2022. University of Porto: Porto, Portugal.

Mustapa, M.A., Yaakob, O., Ahmed, Y.M., Rheem, C.-K., Koh, K., Adnan, F.A., 2017. Wave energy device and breakwater integration: a review. Renew. Sustain. Energy Rev. 77, 43–58.

Neill, S.P., Litt, E.J., Couch, S.J., Davies, A.G., 2009. The impact of tidal stream turbines on large-scale sediment dynamics. Renew. Energy 34 (12), 2803–2812.

Ngo, D.-V., Kim, Y.-J., Kim, D.-H., 2023. Risk assessment of offshore wind turbines suction bucket foundation subject to multi-hazard events. Energies 16. https://doi.org/10.3390/en16052184.

Ni, X., Xue, L., 2020. Experimental investigation of scour prediction methods for offshore tripod and hexapod foundations. J. Mar. Sci. Eng. 8 (11), 856.

Pagliara, S., Carnacina, I., Cigni, F., 2011. Sills and gabions as countermeasures at bridge pier in presence of debris accumulations. J. Hydraul. Res. 49, 764.

Qi, W.-G., Li, Y.-X., Xu, K., Gao, F.-P., 2019. Physical modelling of local scour at twin piles under combined waves and current. Coast Eng. 143, 63–75.

Rosa-Santos, P., Taveira-Pinto, F., Rodríguez, C.A., Ramos, V., López, M., 2019a. The CECO wave energy converter: recent developments. Renew. Energy 139, 368–384.

Rosa-Santos, P., Taveira-Pinto, F., Clemente, D., Cabral, T., Fiorentin, F., Belga, F., Morais, T., 2019b. Experimental study of a hybrid wave energy converter integrated in a harbor breakwater. J. Mar. Sci. Eng. 7 (2), 33.

Rudolph, D., Bos, K.J., Luijendijk, A., Rietema, K., Out, J., 2004. Scour around offshore structures-analysis of field measurements. In: Proceedings 2nd International Conference on Scour and Erosion (ICSE-2). *November 14.–17., 2004, Singapo*re. 2004.

Ruehl, K., Forbush, D., Lomonaco, P., Bosma, B., Simmons, A., Gunawan, B., Bacelli, G., Michelén Ströfer, C., 2019. Experimental Testing of a Floating Oscillating Surge Wave Energy Converter.

Saathoff, J.-E., Goldau, N., Achmus, M., Schendel, A., Welzel, M., Schlurmann, T., 2024. Influence of scour and scour protection on the stiffness of monopile foundations in sand. Appl. Ocean Res. 144, 103920.

Saeidtehrani, S., Fazeres-Ferradosa, T., Rosa-Santos, P., Taveira-Pinto, F., 2022. Review on floating wave-wind energy converter plants: nonlinear dynamic assessment tools. Sustain. Energy Technol. Assessm 54, 102753.

Sánchez, S., López-Gutiérrez, J.-S., Negro, V., Esteban, M.D., 2019. Foundations in offshore wind farms: evolution, characteristics and range of use. Analysis of main dimensional parameters in monopile foundations. J. Mar. Sci. Eng. 7 https://doi.org/10.3390/jmse7120441.

Sarmiento, J., Guanche, R., Iturrioz, A., Ojanguren, T., Ávila, A., Yanes, C., 2021. Experimental evaluation of dynamic rock scour protection in morphodynamic environments for offshore wind jackets. Energies 14 (12), 3379.

Schendel, A., 2018. *Wave-current-induced Scouring Processes And Protection by Widely Graded Material*. 2018. Leibniz University Hannover, Germany.

Schendel, A., Goseberg, N., Schlurmann, T., 2014. Experimental study on the performance of coarse grain materials as scour protection. Coastal Engin. Proceed. 1 (34), 58.

Schendel, A., Goseberg, N., Schlurmann, T., 2016. Erosion stability of wide-graded quarry-stone material under unidirectional current. J. Waterw. Port, Coast. Ocean Eng. 142 (3), 04015023.

Schendel, A., Goseberg, N., Schlurmann, T., 2018. Influence of reversing currents on the erosion stability and bed degradation of widely graded grain material. Int. J. Sediment Res. 33 (1), 68–83.

Schendel, A., Welzel, M., Schlurmann, T., Hsu, T.-W., 2020. Scour around a monopile induced by directionally spread irregular waves in combination with oblique currents. Coast Eng. 161, 103751.

Singh, N.B., Devi, T.T., Kumar, B., 2022. The local scour around bridge piers—a review of remedial techniques. ISH J. Hydraulic Eng 28 (Suppl. 1), 527–540.

Sørensen, S.P.H., Ibsen, L.B., 2013. Assessment of foundation design for offshore monopiles unprotected against scour. Ocean Eng. 63, 17–25.

Soulsby, R.L., 1997. Dynamics of Marine Sands, a Manual for Practical Applications. Thomas Telford Publications, p. 256.

Srisuwan, C., Rattanamanee, P., 2015. Modeling of Seadome as artificial reefs for coastal wave attenuation. Ocean Eng. 103, 198–210.

Stahlmann, A., 2013. Numerical and experimental modeling of scour at foundation structures for offshore wind turbines. In: *The Twenty-Third International Offshore And Polar Engineering Conference*. 2013. OnePetro.

Stahlmann, A., 2014. Numerical and Experimental Modeling of Scour at Foundation Structures for Offshore Wind Turbines, vol. 1, pp. 131–138.

Stahlmann, A., Schlurmann, T., 2010. Physical modeling of scour around tripod foundation structures for offshore wind energy converters. In: Proceedings of the Coastal Engineering Conference. American Society of Civil Engineers, Reston, p. 2010, 2010.

Stroescu, I.E., 2018. Scour development around mono bucket foundations. In: *The Faculty Of Engineering And Science*. 2018. Aalborg University, Aalborg Universitetsforlag.

Stroescu, I., Frigaard, P., 2016. Scour properties of mono bucket foundation. In: Proc., 8th Int. Conf. On Scour and Erosion, vol. 2016.

Sturm, H., 2017. Design aspects of suction caissons for offshore wind turbine foundations. In: Unearth the Future, Connect beyond. Proceedings of the 19th International Conference on Soil Mechanics and Geotechnical Engineering, vol. 2017.

Sumer, B.M., Fredsøe, J., 1997. Hydrodynamics around cylindrical structures, 12. World Scientific, p. 530.

Sumer, B.M., Fredsøe, J., 2001. Scour around pile in combined waves and current. J. Hydraul. Eng. 127 (5), 403–411.

Sumer, B.M., Kirca, V.S.O., 2022. Scour and liquefaction issues for anchors and other subsea structures in floating offshore wind farms: a review. Water Sci. Eng. 15 (1), 3–14.

Sumer, B.M., Fredsøe, J., 2002. The mechanics of scour in the marine environment, 17. World Scientific, p. 536.

Sumer, B.M., Fredsøe, J., Christiansen, N., 1992. Scour around vertical pile in waves. J. Waterw. Port, Coast. Ocean Eng. 118 (1), 15–31.

Sumer, B.M., Whitehouse, R.J.S., Tørum, A., 2001. Scour around coastal structures: a summary of recent research. Coast Eng. 44 (2), 153–190.

Sumer, B.M., Bundgaard, K., Fredsoe, J., 2005. Global and local scour at pile groups. In: 15th International Ocean and Polar Engineering Conference (ISOPE), vol. 2005. Seoul, Korea.

Sun, C., Lam, W.H., Cui, Y., Zhang, T., Jiang, J., Guo, J., Ma, Y., Wang, S., Tan, T.H., Chuah, J.H., 2018. Empirical model for Darrieus-type tidal current turbine induced seabed scour. Energy Convers. Manag. 171, 478–490.

Taheri, O., Kolahdoozan, M., Faghihirad, S., 2022. Experimental study of bed level changes in the vicinity of flap-type wave energy converters. Ships Offshore Struct. 1–12.

Tang, Z.-H., Melville, B., Singhal, N., Shamseldin, A., Zheng, J.-H., Guan, D.-W., Cheng, L., 2022. Countermeasures for local scour at offshore wind turbine monopile foundations: a review. Water Sci. Eng. 15 (1), 15–28.

Taveira-Pinto, F., Rosa-Santos, P., Fazeres-Ferradosa, T., 2021. Recent work and prospective analysis on offshore structures and marine energy harvesting at the Faculty of Engineering of the University of Porto. In: IOP Conference Series: Materials Science and Engineering, vol. 2021. IOP Publishing.

Tavouktsoglou, N.S., 2018. Scour and Scour Protection Around Offshore Gravity Based Foundations. UCL (University College London), 2018.

Vahdati, V.J., Yaghoubi, S., Torabipour, A., Correia, J.A.F.O., Fazeres-Ferradosa, T., Taveira-Pinto, F., 2020. Combined solutions to reduce scour around complex foundations: an experimental study. Marine Syst. Ocean Technol. 15 (1), 81–93.

Van Der Meer, J.W., 1990. Rock Slopes and Gravel Beaches under Wave Attack. TU Delft: Delft Hydraulics Publications, 1990.

Van Velzen, G., Bruinsma, N., 2017. Scour Development and Conceptual Scour Protection Layout at HKZ Hollandse Alpha and Beta, 2017, Deltares.

Van Velzen, G., Riezebos, H., Bruinsma, N., 2016. OHVS - Scour and Scour Prediction. Physical Modelling Test Programme, Deltares, 2016.

Wang, X., Zeng, X., Li, J., Yang, X., Wang, H., 2018. A review on recent advancements of substructures for offshore wind turbines. Energy Convers. Manag. 158, 103–119.

Wang, G., Xu, S., Zhang, Q., Zhang, J., 2023a. An experimental study of the local scour protection methods around the monopile foundation of offshore wind turbines. Ocean Eng. 273, 113957.

Wang, W., Yan, J., Chen, S., Liu, J., Jin, F., Wang, B., 2023b. Gridded cemented riprap for scour protection around monopile in the marine environment. Ocean Eng. 272, 113876.

Welzel, M., 2021. Wave-current-induced Scouring Processes Around Complex Offshore Structures. Leibniz Universität, Hannover, Germany, 2021.

Welzel, M., Schendel, A., Hildebrandt, A., Schlurmann, T., 2019a. Scour development around a jacket structure in combined waves and current conditions compared to monopile foundations. Coast Eng. 152, 103515.

Welzel, M., Schendel, A., Schlurmann, T., Hildebrandt, A., 2019b. Volume-based assessment of erosion patterns around a hydrodynamic transparent offshore structure. Energies 12 (16), 3089.

Welzel, M., Schendel, A., Goseberg, N., Hildebrandt, A., Schlurmann, T., 2020. Influence of structural elements on the spatial sediment displacement around a jacket-type offshore foundation. Water 12 (6), 1651.

Welzel, M., Schendel, A., Satari, R., Neuweiler, I., Schlurmann, T., 2024. Spatio-temporal analysis of scour around complex offshore foundations under clear water and live bed conditions. Ocean Eng. 298, 117042.

Whitehouse, R.J.S., 1998. Scour at Marine Structures : a Manual for Practical Applications. Thomas Telford, London.

Whitehouse, R.J.S., Harris, J.M., Sutherland, J., Rees, J., 2011a. The nature of scour development and scour protection at offshore windfarm foundations. Mar. Pollut. Bull. 62 (1), 73–88.

Whitehouse, R.J.S., Sutherland, J., Harris, J.M., 2011b. Evaluating scour at marine gravity foundations. Proc. Inst. Civ. Eng.: Maritime Engineering 164 (4), 143–157.

Wilms, M., Stahlmann, A., Schlurmann, T., 2012. Investigations on scour development around a gravity foundation for offshore wind turbines. In: Proceedings of the Coastal Engineering Conference (2012). American Society of Civil Engineers, Reston, 2012.

WindEurope, 2021a. Getting fit for 55 and set for 2050: electrifying Europe with wind energy, 2021 WindEurope. Belgium.

WindEurope, 2021b. Offshore wind in Europe - key trends and statistics 2020. WindEurope: Belgium, 2021.

WindEurope, 2022a. *Financing and investment trends 2021: the European wind industry in 2021*. 2022. WindEurope. Belgium.

WindEurope, 2022b. Wind energy in Europe: 2021 statistics and the outlook for 2022-2026, 2022 WindEurope. Belgium.

Xiao, Y., Jia, H., Guan, D., Liang, D., Yuan, S., Tang, H., 2020. Experimental investigation on scour topography around high-rise structure foundations. Int. J. Sediment Res. 36.

Xiao, Y., Jia, H., Guan, D., Liang, D., Yuan, S., Tang, H., 2021. Modeling clear-water scour around the high-rise structure foundations (HRSF) of offshore wind farms. J. Coast Res. 37.

Yagci, O., Yildirim, I., Celik, M.F., Kitsikoudis, V., Duran, Z., Kirca, V.S.O., 2017. Clear water scour around a finite array of cylinders. Appl. Ocean Res. 68, 114–129.

Yang, B., Wei, K., Yang, W., Li, T., Qin, B., 2021. A feasibility study of reducing scour around monopile foundation using a tidal current turbine. Ocean Eng. 220, 108396.

Yin, Q., Xing, X., Wang, W., Zhai, J., Xu, S., 2023. Effect of scour erosion and riprap protection on horizontal bearing capacity and reliability of monopiles using FEM-BPNN-RSM coupled method. Appl. Ocean Res. 140, 103720.

Yu, T., Zhang, Y., Zhang, S., Shi, Z., Chen, X., Xu, Y., Tang, Y., 2019. Experimental study on scour around a composite bucket foundation due to waves and current. Ocean Eng. 189, 106302.

Zhang, F., Chen, X., Feng, T., Wang, Y., Liu, X., Liu, X., 2022. Experimental study of grouting protection against local scouring of monopile foundations for offshore wind turbines. Ocean Eng. 258, 111798.

Zhang, F., Xuguang, C., Jiahao, Y., Xingzheng, G., 2023. Countermeasures for Local Scour Around Offshore Wind Turbine Monopile Foundations: A Review, 103764.

Zhao, F., Yang, M., Tang, Y., Xu, S., 2023. Numerical simulation of offshore wind power pile foundation scour with different arrangements of artificial reefs. Front. Mar. Sci. 10, 1178370.

Zhu, Y., Xie, L., Su, T.-C., 2020. Scour protection effects of a geotextile mattress with floating plate on a pipeline. Sustainability 12 (8), 3482.